

Alma Mater Studiorum – Università di Bologna

**DOTTORATO DI RICERCA IN  
SCIENZE BIOMEDICHE**

Ciclo XXIX

**Settore Concorsuale di afferenza: 06/A4**

**Settore Scientifico disciplinare: MED/08**

**NEW FRONTIERS OF SKIN TISSUE ENGINEERING:  
FROM THE LABORATORY TO CLINICAL PRACTICE**

**Presentata da:**

**Martina Ghetti**

**Coordinatore Dottorato:**

**Prof. Lucio Ildebrando Cocco**

**Relatore:**

**Prof.ssa Giovanna Cenacchi**

**Co-relatore:**

**Dott.ssa Elena Bondioli**

**Esame finale anno 2017**



# Contents

---

SUMMARY .....	5
1. INTRODUCTION.....	7
1.1 Morpho-functional aspects of the skin.....	7
1.1.1 Functions of the epidermis .....	7
1.1.2 Heterogeneity of skin cells.....	7
1.1.3 Dermal fibroblasts as the main cell type responsible for extracellular matrices synthesis.....	10
1.1.4 Extracellular matrix (ECMs) composition .....	11
1.2 Regeneration ability of the skin: wound healing process.....	12
1.2.1 Role of different fibroblast populations in wound healing.....	13
1.2.2 Extracellular matrix (ECMs) influences in wound healing.....	14
1.3 Skin regeneration in vitro: tissue engineering.....	15
1.3.1 Products used for treatment of wounds .....	16
1.4 Human Decellularized Dermal Matrix (HDM) produced by Regional Skin Bank.....	18
1.4.1 Clinical applications of Human Decellularized Dermal Matrix (HDM).....	20
1.5 Abdominal Wall Defects and common treatments.....	21
1.5.1 Biomaterials for Abdominal Wall Defects.....	21
2. AIMS OF THE THESIS .....	23
2.1 Differences in fibroblast extracellular matrices (ECMs) and their role in supporting keratinocytes growth and basement membrane formation.....	23
2.2 Investigation of Human Decellularized Dermal Matrix (HDM) regenerative ability in the reconstruction of Abdominal Wall Defects.....	24
3. MATERIALS AND METHODS .....	27
3.1 Differences in fibroblast extracellular matrices (ECMs) and their role in supporting keratinocytes growth and basement membrane formation.....	27
3.1.1 Human tissue samples and cell culture .....	27
3.1.2 ECMs generation.....	28

---

3.1.3	ECMs analysis.....	30
3.1.4	Generation of epidermal only skin constructs.....	33
3.1.5	Skin constructs analysis: viability and basement membrane formation.....	34
3.1.6	Graphs and statistical analysis.....	35
3.2	Investigation of Human Decellularized Dermal Matrix (HDM) regenerative ability in the reconstruction of Abdominal Wall Defects.....	36
3.2.1	Tissue procurement.....	36
3.2.2	Patient population and surgical procedure.....	36
3.2.3	Histological and ultrastructural analysis of HDM biopsy specimens.....	38
4.	RESULTS AND DISCUSSION.....	41
4.1	Differences in fibroblast extracellular matrices (ECMs) and their role in supporting keratinocytes growth and basement membrane formation.....	41
4.1.1	ECMs thickness and morphology.....	42
4.1.2	ECMs composition.....	43
4.1.3	Skin constructs analysis.....	47
4.2	Investigation of Human Decellularized Dermal Matrix (HDM) regenerative ability in the reconstruction of Abdominal Wall Defects.....	51
4.2.1	Patients clinical follow-up.....	51
4.2.2	Histological and ultrastructural findings of HDM biopsy specimens.....	54
5.	CONCLUSIONS.....	61
6.	REFERENCES.....	65

# SUMMARY

---

This PhD thesis is mainly focused on the key role of extracellular matrix in skin tissue engineering. In the first part I presented three dimensional structures derived through the physiological cell secretion of extracellular matrix (ECM), that may be a bioinspired scaffold. I performed a biological characterization of cell-assembled ECMs from three different sub-populations of fibroblasts found in human skin; papillary fibroblasts (Pfi), reticular fibroblasts (Rfi), and dermal papilla fibroblasts (DPfi). Specifically, fibroblast sub-populations were cultured with ascorbic acid to promote cell-assembled matrix production for 10 days. Subsequently, cells were removed and the remaining matrices were characterized. I found that the ECM assembled by Pfi exhibited randomly oriented fibers, associated with highest interfibrillar space, reflecting ECM characteristics which are physiologically present within the papillary dermis. Mass spectrometry followed by validation with immunofluorescence analysis showed that THROMBOSPONDIN (TSP1) is preferentially expressed within the DPfi derived matrix. Additionally, in another experiment, keratinocytes were seeded on the top of cell depleted ECMs to generate epidermal only skin constructs. I found that epidermal constructs grown on DPfi or Pfi matrices exhibited normal basement membrane formation, while Rfi matrices were unable to support membrane formation. For this reason, inspiration should be taken from these different ECMs, to improve the design of therapeutic biomaterials in skin engineering applications.

---

In the second part, I focused on human decellularized dermal matrices, due to their ability to reduce numerous side effects related to hernia repair. However, only animal studies investigated the biological interaction post-implant of human decellularized matrices for soft tissue repair. Thus, the aims of this second part were to show the clinical results after the application of human decellularized matrix produced by Regional Skin Bank in patients suffering from abdominal hernia and to evaluate the morphologic response one year post implant, through morphological analysis of biopsy specimens. Overall, clinical results showed that all the patients revealed a well tolerability of human decellularized dermal matrix and a normal wound healing was also identified in all the damage areas. Follow up after 6 months reported no signs of dermis rejection and that none of the patients was positive to serological tests. Moreover, histological and ultrastructural results of post-implant biopsy specimens showed a perfect cellular repopulation, neo-angiogenesis, minimal inflammatory response and a well-organized collagen matrix in all biopsies investigated. Thus, this scaffold can be considered a safe and useful product to treat large abdominal defects, characterized by minor complications and simplicity to be implanted.

# 1. INTRODUCTION

---

## 1.1 Morpho-functional aspects of the skin

Skin is the largest and one of the most complex organ in the human body, that consists of a multi-layered structure comprising of an underlying supporting dermis and functional epithelium at the skin surface. In particular, the epidermis is a highly specialized epithelium that has evolved to perform multiple essential protective functions, for this reason skin cellular components must remain dynamic to allow tissue regeneration and response to cutaneous insults [1].

### 1.1.1 *Functions of the epidermis*

The skin is highly specialized because it provides a barrier function through the prevention of water loss, the resistance to mechanical stimuli and the protection against physical, chemical and/or biological agents such as temperature, light, chemicals, toxins and micro-organisms. In addition to the first function, it plays a role in sensation, thermoregulation, excretion, absorption, pigmentation and innate/acquired immunity. When this barrier is disrupted due to any cause- surgery, ulcers, burns, neoplasms or traumas- the functions of the skin are no longer adequately performed. Therefore, it is crucial to restore the integrity of the skin as soon as possible [2].

### 1.1.2 *Heterogeneity of skin cells*

Within each layer of the skin there are multiple cells with different functions which contribute to tissue homeostasis. The most abundant cell type within the epidermis are

---

the keratinocytes; these differentiate and stratify towards the skin surface equipping skin with its barrier function. Specifically, it consists of five layers where stratum basale, the deepest layer adjacent to the basal lamina, contains the dividing cells. The other layers are named stratum spinosum, stratum granulosum, stratum lucidum and stratum corneum (Figure 1). Moreover, the epidermis also contains melanocytes (pigment cells), Merkel's cells (sensory cells) and immature dendritic cells known as Langerhans cells (immunological cells).

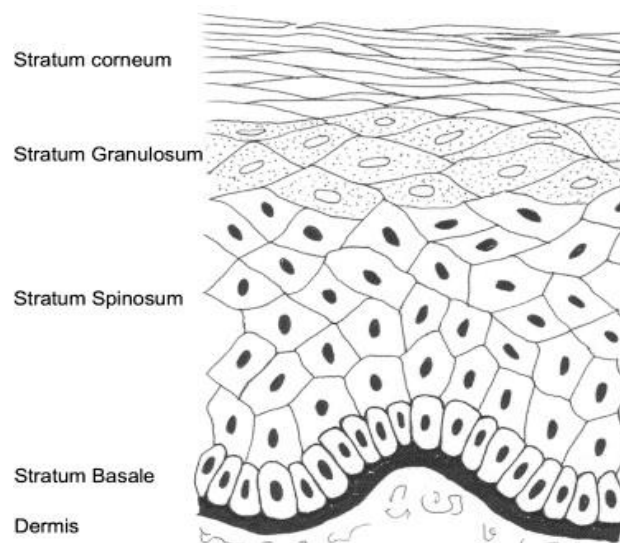


**Figure 1:** Drawing of normal human epidermis showing the different layers [3].

The dermis is a highly specialized and dynamic tissue organized in two main layers. Papillary dermis is the superficial portion of the dermis that lies immediately beneath the epidermis and contains the rete ridges. It is demarcated from the underlying reticular dermis by a vascular plexus and below rests the hypodermis. The deeper portion of the dermis, reticular dermis, is mainly responsible for anchoring of skin appendages (i.e. hair, erector-pili muscles, sebaceous glands, and sweat glands) but also gives strength to the dermal layer [2].

Within the dermis there are actually several types of skin fibroblasts (Figure 2), whose primary role is to secrete components of the extracellular matrix (ECM), which can be defined by their spatial location [4], and exist as morphologically and functionally-heterogeneous sub-populations [5]. For example, the fibroblast population within the dermal layer adjacent to the basement membrane and epidermis known as the papillary dermis are called papillary fibroblasts (Pfi). These are distinct from those residing within the lower reticular dermis, which are termed reticular fibroblasts (Rfi) [6]. In hairy skin there are also fibroblasts associated with the hair follicle, located in the dermal papilla and the connective tissue sheath [7]. Dermal papilla fibroblasts (DPfi) have specialized signalling properties required for hair follicle morphogenesis and coordination of hair growth [8]. These dermal papilla fibroblasts are also derived from the upper (papillary) fibroblasts during skin development (Figure 3). By postnatal day 2 in mouse skin, these three fibroblast populations are committed to their fate, and they contribute to the composition of the skin dermis.

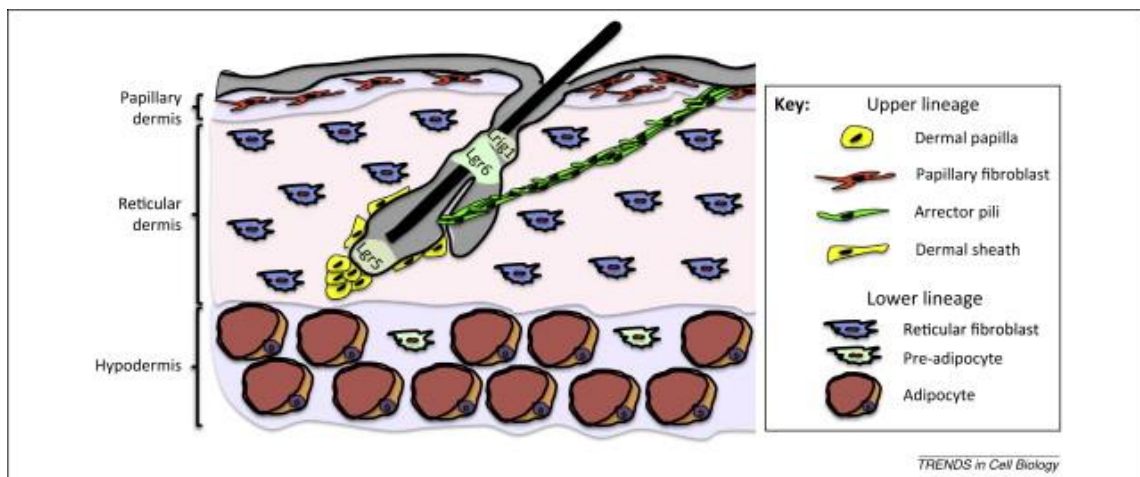


**Figure 2:** Heterogeneity of cells in skin dermis [9].

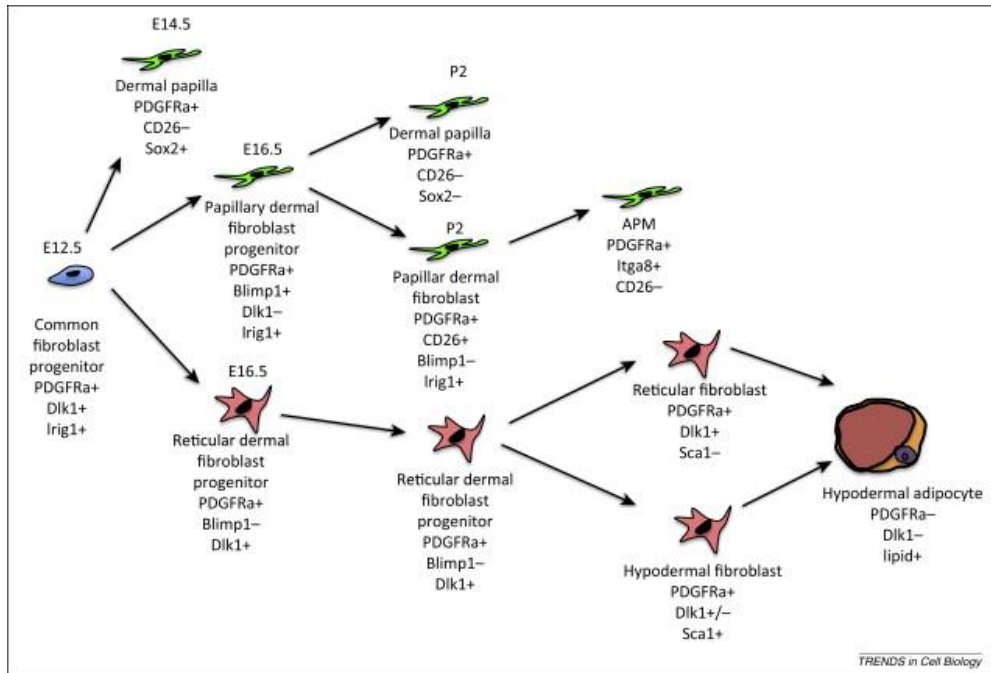


**Figure 3:** Three fibroblast lineages derived from a common cell progenitor dermis [9]

### 1.1.3 *Dermal fibroblasts as the main cell type responsible for extracellular matrices synthesis*

Dermal fibroblasts are a key component of skin; they not only produce and organize the extracellular matrix (ECM) of the dermis but they also interact with each other and other cell types, playing a pivotal role in regulating skin physiology. Various studies have demonstrated that ECMs produced by Pfi and Rfi within the interfollicular dermis are distinct with regard to their composition and architecture [5]. Firstly, Pfi in the upper dermis secrete ECM which is constituted of thin, poorly-organized collagen fiber bundles, while thick well-organized collagen bundles are characteristic within the lower dermis which is produced by resident Rfi. The papillary dermis also has a higher ratio of collagen type-III to I, and higher levels of decorin. By contrast, versican is more extensively expressed in elastic fibers of the reticular dermis [10].

In addition, the non-fibrillar collagen types XII and XVI, along with tenascin-C, are characteristically found in the papillary dermis; whereas, collagen type IV and tenascin-X are primarily restricted to the reticular dermis [11, 12]. Finally the dermal papilla is also rich in interstitial collagens such as type I and type III, in addition to fibrillar matrix proteins such as fibronectin and glycoproteins such as thrombospondin [13].

#### 1.1.4 Extracellular matrix (ECMs) composition

The extracellular matrix can be considered as a dense and complex network of macromolecules with a well-defined and specific biomechanical properties, which regulates cell functions such as growth, differentiation and survival. Cell-ECM adhesion occurs due to integrin receptors placed on the cell membranes, which transmit signals that allow cells to adapt to the surrounding microenvironment. Furthermore, the ECMs release a series of growth factors that have a role in the regulation of different cell functions [14].

The extracellular matrix components can be divided into: fiber forming structural molecules; non fiber forming structural molecules and matricellular proteins that modify cell-matrix interaction (Figure 4) [15].

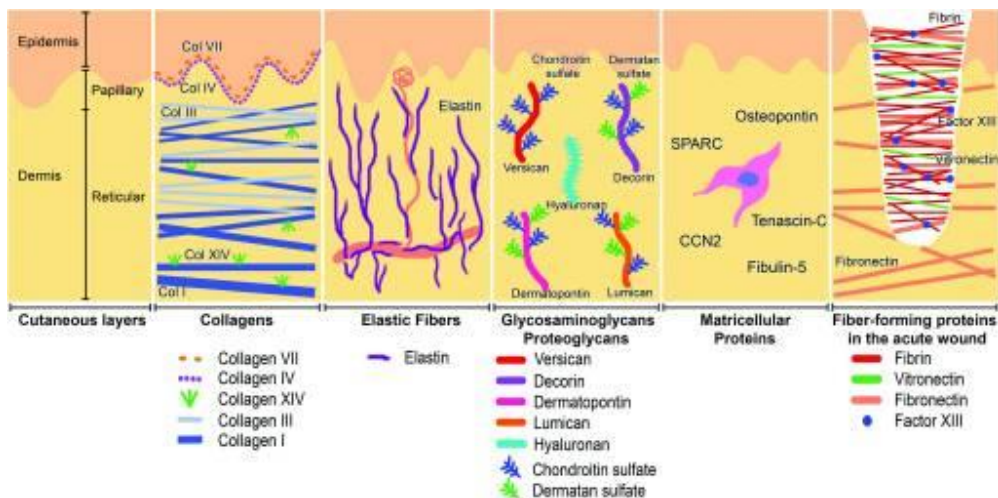


**Figure 4:** ECM composition of normal skin [16].

Fiber-forming molecules provide a structure to the ECM by creating a complex three-dimensional framework of rigid proteins. In particular, collagen is the most abundant fiber-forming protein, which comprises 77% of dry weight of human skin [17]. Other fiber-forming proteins include fibrin, fibronectin, vitronectin, elastin and fibrillin [18]. In contrast, nonfiber-forming structural molecules, mostly proteoglycans and GAGs, fill the majority of the tissue's interstitial space. The most abundant proteoglycans in the skin include hyaluronan (HA), decorin, versican and dermatopontin. Their functions are hydration, buffering and force dispersions within tissues, due to their negatively charged and hydrophilic nature [19]. Also present in the ECM are the matricellular proteins, a group of secreted local proteins that interact in autocrine or paracrine cell-matrix signaling. They include osteopontin, secreted protein, acid and rich in cysteine (SPARC), tenascin-C, fibulins and the CCN family [20].

## **1.2 Regeneration ability of the skin: wound healing process**

Skin healing requires complex interactions between keratinocytes, fibroblasts, ECM and stem cell populations within the basal epidermis, the appendages and underlying mesenchyme in order to repair injured tissues. This involves several cellular activities such as synthesis of collagen and other matrix components, phagocytosis, chemotaxis, and mitogenesis. Under normal conditions, the wound healing process correlates well with the appearance of different cell types in various phases of the wound healing process. Four distinct, but overlapping, phases characterize this process: Haemostasis, Inflammation, Proliferation, and Remodelling (Figure 5) [21].

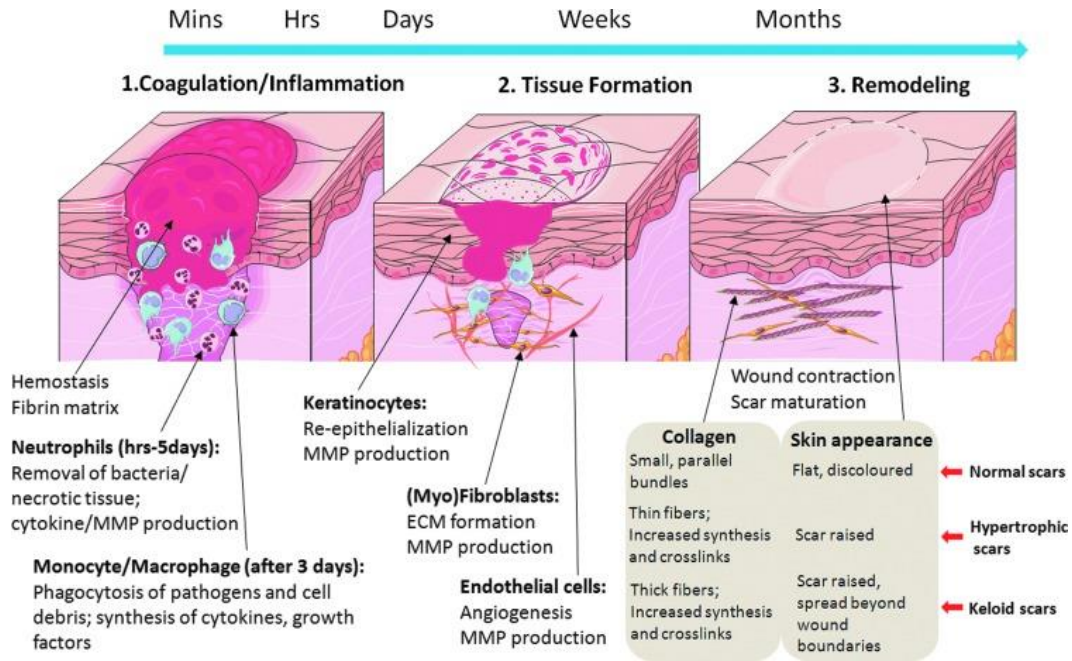


**Figure 5:** Stages of cutaneous wound healing [22].

### 1.2.1 Role of different fibroblast populations in wound healing

The functional heterogeneity of fibroblasts is not only important for skin homeostasis but also for wound healing. Some studies showed that the first wave of dermal repair is mediated by reticular dermis and hypodermis, which are not able of inducing hair follicles. These lower lineage fibroblasts express myofibroblast markers such as  $\alpha$ -SMA and secrete large amounts of ECM proteins such as collagen, characteristics of fibrosis [9]. In contrast, upper dermal fibroblasts are recruited during sub-sequent wound re-epithelisation and can induce hair follicle formation. It is well demonstrated that the activation of Wnt pathway induces formation of new hair follicles, fibroblast proliferation and dermal ECM remodelling [6]. To understand fibroblast behavior within the skin is important, especially in the context of wounding, if we want to successfully modulate this process.

### ***1.2.2 Extracellular matrix (ECMs) influences in wound healing***

The ECM remodeling is the latter of a dynamic series of physiological events, which happen when a cutaneous injury occurs. During wound healing, ECM proteins are degraded by proteolytic enzymes, inducing local release of growth factors such as fibroblast growth factors, TGF- $\beta$ , vascular endothelial growth factor, epidermal growth factor, and bone morphogenetic proteins from their insoluble anchorage, consisting of fibronectin, collagens, proteoglycans, heparin and heparin sulphate. In addition, recent studies also demonstrate that ECM proteins are key components in shaping the stem cell niche to maintain stem cell homeostasis and to direct lineage commitment [23]. ECM composition in the dermis alters after wound healing. This involves that the normal matrix is gradually replaced by a denser matrix composed mainly of collagen. Basically, the most significant difference between normal tissue and scar tissue seems to be the orientation of the fibrous matrix [24]. In human scars, the collagen forms cross-links to align in a single direction parallel to the skin, and there is larger fiber size. During the early stages of granulation tissue formation, myofibroblasts deposit collagen III, which plays a role in fibrillogenesis and determines the fibril diameter of collagen I [25]. Eventually myofibroblasts become surrounded by fibrillar collagen which causes arrest in G1 phase of their cycle and a reduction in their ability to adhere to ECM due to the disassembly of cellular focal adhesions [26]. For these reasons targeting components of the ECM during wound repair provides an attractive approach to avoid abnormal scars.

### 1.3 Skin regeneration in vitro: tissue engineering

The role of Skin Tissue Engineering in the field of Regenerative Medicine has been the topic of substantial research over the past three decades. Specifically, Skin Tissue Engineering is a multidisciplinary research area based on the understanding of skin structure, skin mechanics and tissue formation to induce new functional tissues. Three main pillars of tissue engineering were identified (Figure 6): a scaffold provides a structure for tissue growth, while cells produce the desired extracellular matrix under different signals able to affect their growth and phenotype [27].

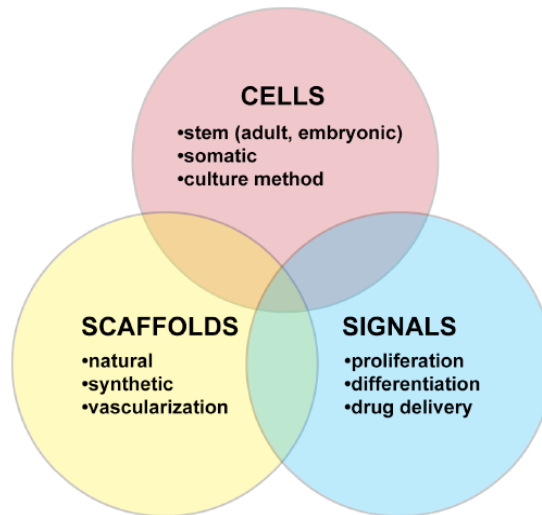


**Figure 6:** Scheme of the three pillars of tissue engineering. To bring tissue engineering into reality, it is crucial to combine the three [27].

Injured skin can normally promote self-healing thanks to the presence of basal layer epidermal stem cells. However in deep injuries, negative regulation of wound healing process may lead to the formation of chronic wounds [28]. These non-healing wounds account for 2-4% of the health care budget in industrialized countries, with 1% of the population affected by such a wound at any time. For these reasons, development of effective treatments is a major unmet medical need [29]. The gold standard treatment

for these wounds such as burns was a split thickness autograft, taken from an uninjured donor site on the patient. Nevertheless they were often limited by the poor availability of healthy tissues [30]. In these cases, clinical application of tissue engineered skin substitutes is the best strategy to overcome the problems related to autograft. Indeed there are a number of biological products available on the market which promote healing, and have been developed combining primary skin cells together with biomaterials.

The development of artificial materials or skin grafts grown in the laboratory for skin replacement has been an area of particular interest over the past two decades. In deep wounds, an 'ideal' skin substitute would provide immediate replacement of both epidermis and dermis layers. Therefore, the ideal skin substitute is nontoxic, has little or no antigenicity, is immunologically compatible, and does not transmit disease. In addition, it is conformable to irregular wound surfaces, flexible and durable, closes the wound immediately and it is bio-absorbable. Finally it facilitates early motion; and provides coverage of vessels, tendons, and nerves to prevent desiccation [31].

### ***1.3.1 Products used for treatment of wounds***

There are a number of biological products available on the market which promote healing. Early studies carried out by Rheinwald & Green (1975), and Yannas & Burke (1980) formed the basis for the development of future skin replacements [32]. Depending on their composition, both synthetic and biological skin substitutes can be divided into dermal, epidermal or dermo-epidermal replacements (Figure 7) [28]. In particular, there are a small number of bioengineered skin products that replace both the epidermis and dermal part of the skin, and one such example is Apligraf<sup>®</sup>, which is

composed of neonate-derived fibroblasts cultured in a bovine collagen matrix, over which neonate-derived keratinocytes are seeded to produce a stratified epidermis [33].

In recent years, a group of biological scaffolds comprised of ECMs which are used solely as a dermal replacement have gained increasing interest. Their main feature is to maintain their own three-dimensional structure for a minimum of three weeks to allow in-growth of blood vessels and fibroblasts, as well as coverage by epithelial cells. One of these is Integra<sup>®</sup>, a dermal regeneration template composed of a layer of bovine tendon collagen type I matrix and shark chondroitine-6-sulfate juxtaposed against a silicone layer that acts as a temporary pseudo-epidermis [34].

Despite the success of Integra, there are some limitations. An alternative to this is MatriDerm<sup>®</sup>, which is an engineered dermal template specially developed to provide a one-step grafting procedure. Matriderm<sup>®</sup> is a scaffold consisting of a native bovine type I, III and V collagen fibre template incorporating elastin hydrolysate that is converted into native host collagen within weeks following application [35]. In addition to engineered scaffolds, human decellularized dermal matrices (HDM) from cadaveric donors is now becoming more popular as a scaffold for use after injury [36]. Also, decellularized skin dermis from cadaveric donor is now becoming more popular as a scaffold. The common feature of all these dermal scaffolds is that the native collagen fibres form a scaffold that guides fibroblasts and possibly other cells toward dermal regeneration, while the presence of elastin particles in the collagen matrix diminishes the formation of granulation tissue in the early phase of wound healing. As a result, a high-quality neoderms with randomly organised collagen bundles is regenerated.

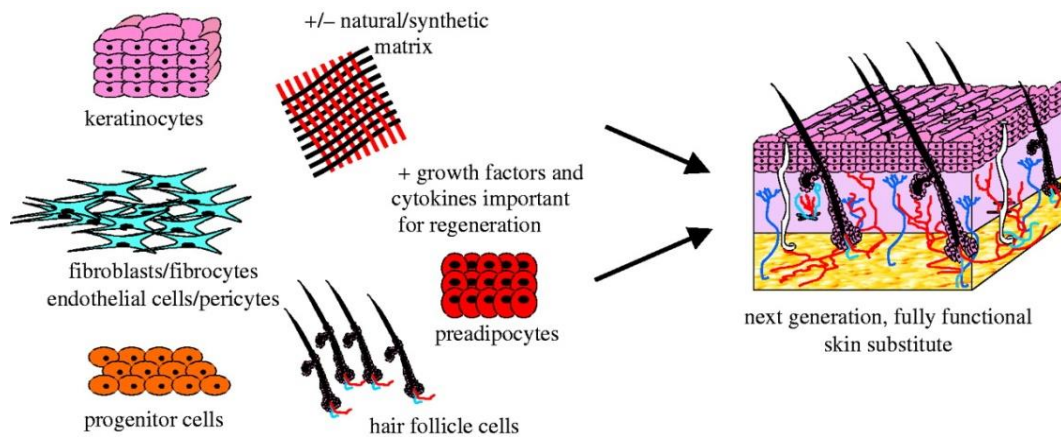


**Figure 7:** Schematic representation of skin substitutes' preparation [32].

#### **1.4 Human Decellularized Dermal Matrix (HDM) produced by Regional Skin Bank**

Nowadays interest is increasing for human decellularized scaffolds, from human cadaveric donors obtained through decellularization processes of dermis or fascia lata, for their ability to favor the healing and cell infiltration after transplantation, with no sign of rejection [37]. These human decellularized matrices are classified as human tissues for transplantation and each Country has to follow National Regulatory Transplantation Center rules for the control of human-derived tissue transplants [38].

In 2008, Emilia-Romagna Regional (RER) Skin Bank of Bufalini Hospital in Cesena in collaboration with Rizzoli Orthopedic Institute in Bologna, produced a cell-free scaffold, totally biocompatible and safe starting from skin of cadaveric donor, patenting a decellularization method able to remove cellular components from dermal tissue (Figure 8). This scaffold has the potential to interact with the surrounding host tissues, maintaining biomechanical strength and biochemical components [36].

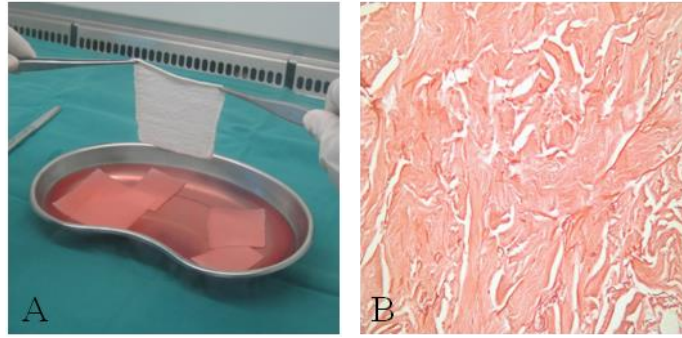


**Figure 8:** Human decellularized dermis (HDM) produced by RER Skin Bank. (A) Gross anatomy of HDM after the patented decellularization procedure. (B) Histological staining of HDM shows intact collagen fibers and bundles with no cellular materials (H&E, original magnification 20x).

Specifically, from 2008 to 2010, human dermis was taken from the backs of 57 multi-organ and/or multi-tissue donors following national rules on harvesting, processing and distributing tissues for transplantation (CNT 09/2016), and decellularized at the Skin Bank. Firstly, in sterile conditions, using an electric dermatome, the epidermis was separated from the dermis trunk area and discarded, then 10–20 cm<sup>2</sup> dermis samples were dissected. The dermis grafts were then rinsed with 0.9% NaCl solution and stored in this solution for transport (at 2–4 °C) to the treatment station (< 12 h), where they were aseptically submitted to a chemical and physical treatment of decellularization. Finally, the dermis was submitted to irradiation with  $\gamma$ -rays (100Gy) and stored in nitrogen vapor at 180 °C to 190 °C. Membrane cellularity, morphology, bioactivity, biomechanical properties and in vivo biocompatibility were assessed before starting with the clinical applications of HDM with the approval of the Hospital Ethical Committee.

#### ***1.4.1 Clinical applications of Human Decellularized Dermal Matrix (HDM)***

Human Decellularized Dermal Matrices (HDMs) are currently applied in different clinical fields such as orthopedic surgeries, dental and craniomaxillofacial repairs, soft tissue reconstruction, and wound healing [39]. Orthopedic surgeons commonly use HDMs in soft tissue repair procedures to provide additional biomechanical strength and improve healing for rotator cuff repairs, especially for large and massive tears [40, 41]. In addition, HDM is applied to augment Achilles tendon for increased biomechanical strength [42]. HDM is also able to facilitate bone regeneration [43] and soft tissue alveolar ridge augmentation [44] after a tooth extraction, which usually requires immediate ridge augmentation to prevent further resorption, affecting the placement of dental implants. Another important clinical application is the treatment of acute and chronic wounds. In particular non-healing, diabetic ulcers of the lower limbs can be treated with an HDM to achieve complete healing and integration while avoiding second site morbidity [45]. Burns treatment has also achieved good outcomes with reduced scarring, revascularization and recellularization [46]. Finally, soft tissue reconstruction procedures of the breast and abdominal wall defects commonly utilize HDMs.

## **1.5 Abdominal Wall Defects and common treatments**

Abdominal wall defects are unusual abdomen openings and can be caused by trauma, burns, treatment of abdominal compartment syndrome and resection of abdominal tumors [47]. Although these defects result as one of the most common surgical procedures performed every year, they still lead to high mortality rate and represent a major challenge for plastic and reconstructive surgeons. Different methods for the repair of abdominal wall defects have been described including the use of autogenous fascial flaps as well as prosthetic implantable materials [48-50]. In particular, the implantation of synthetic biocompatible materials generally allowed a decreased recurrence rate of incisional hernia due to their high tensile strength and reconstructive abilities [51-53]. However, several side effects may be related to the implantation of synthetic biomaterials, including immunological reaction, bowel adhesions, fistula formation, surgical site infections or mesh extrusion [54]. In order to avoid these complications, in recent decades several biological scaffolds have been designed for abdominal wall defects repair, reducing problems of tolerability and acceptability compared to synthetic materials [55].

### ***1.5.1 Biomaterials for Abdominal Wall Defects***

The birth of biologic materials, such as human decellularized dermal matrix (HDM), has changed the standard treatment of infected and/or complex abdominal wall defects. Nowadays, most reconstructions of these conditions are performed using biologic materials as the substrate for tension-free closure. A number of reports have documented the efficacy of HDM as a graft material for the repair of acquired abdominal wall defects, with promising results [56]. These biomaterials have been shown to become recellularized and revascularized in both animal and human subjects.

They contain collagen and elastin, hyaluronan, proteoglycans, fibronectin, the most important components of the extracellular matrix. In addition, HDM has the mechanical properties (i.e., tensile strength and elasticity) of a mesh for abdominal wall reconstructions. Nevertheless, once repopulated with a vascular network, the graft material is theoretically able to clear bacteria from the wound bed site through the release of inflammatory cells as well as nutrients and oxygen, a property not found in prosthetic graft materials. Finally, unlike autologous materials such as fascial grafts and muscle flaps, acellular dermal matrix can be used without subjecting the patient to additional morbidity in the form of donor site complications [57].

## 2. AIMS OF THE THESIS

---

### 2.1 Differences in fibroblast extracellular matrices (ECMs) and their role in supporting keratinocytes growth and basement membrane formation

After injury or in the case of a chronic skin wound, there are a number of biological products available on the market which promote healing. In particular, human decellularized dermal matrices (HDM) from cadaveric donor are now becoming more popular as a scaffold. The common feature of all these dermal scaffolds is that a high-quality neoderms with randomly organized collagen bundles is regenerated. However, these decellularized dermal scaffolds are commonly taken from reticular dermis rather than papillary dermis. Reticular dermis is much thicker than papillary dermis, and therefore provides a greater area for cell infiltration. In addition, its relatively low cellularity in comparison to the papillary dermis means it is easy to decellularize. Lastly, the reticular dermis shows a strong mechanical resistance when compared to papillary dermis making it easy to handle. Despite these advantages, decellularized reticular dermis does not have a basal membrane and this feature can make re-epithelization of grafts by host keratinocytes cells more difficult. For these reasons, the problem of dermal scaffolds is they do not reflect the heterogeneity observed within the skin dermis, where different fibroblast sub-populations, have divergent functions. Furthermore, with decellularized scaffolds, in particular of animal origin, there can be issues associated with inflammation, and these

---

foreign body reactions have lead scientists to investigate new strategies based on in vitro organogenesis approaches. A therapeutic strategy such as this requires cells to first be obtained from their native tissue, then kept in long term culture with appropriate growth factors to produce a tissue substitute rich in ECM. Based on the above observations, I decided to investigate cell derived ECMs as potential scaffolds for use in skin tissue engineering. Thus, the two main objectives of this first part of the thesis were:

- 1) to generate and biologically characterize cell-assembled ECMs produced by fibroblast sub-populations found both with the hair follicle dermis and the papillary and reticular dermis of human skin.
- 2) to evaluate how ECMs from fibroblasts in different dermal locations, which are from areas juxtaposed to basement membrane, or devoid of basement membrane, can interact with and instruct basement membrane formation in epithelial only skin constructs.

## **2.2 Investigation of Human Decellularized Dermal Matrix (HDM) regenerative ability in the reconstruction of Abdominal Wall Defects**

Human decellularized membranes are currently the subject of intense study, especially due to their ability to promote tissue regeneration. On this basis, the ideal scaffold for abdominal wall defects should be easily implanted with minimal patient morbidity, while assisting the long-term recovery of the tissue functionality. Moreover, the absence of inflammation, the quality of connective tissue organization, cellular repopulation as well as new tissue ingrowth and neo-angiogenesis represent

other features for the ideal scaffold for soft tissue regeneration. To my knowledge, only animal studies investigated the *in vivo* biological interaction post-implant of scaffolds for soft tissue repair, while, it was noted the difficulty in obtaining a post-surgery biopsy specimens. In this respect, the success of the graft is usually established only by non-invasive analysis and functional outcomes measures. However, the post-implant evaluation would offer key information about the incorporation of the graft and the host cellular response in the human.

Thus, the two main aims of this second part of the thesis were:

- 1) to show the clinical results obtained after the application of human decellularized dermal matrix, produced by RER Skin Bank, on patients suffering from different abdominal wall defects.
- 2) to evaluate the morphologic response at 1 year post implantation of human decellularized dermal matrix (HDM), through histological and ultrastructural analysis of biopsy specimens.



## 3. MATERIALS AND METHODS

---

### 3.1 Differences in fibroblast extracellular matrices (ECMs) and their role in supporting keratinocytes growth and basement membrane formation

#### 3.1.1 *Human tissue samples and cell culture*

Scalp skin tissue were taken from healthy donors using REC approved consent forms and used for the isolation of epidermal keratinocytes, and dermal sub-populations. Specifically, Pfi and Rfi were obtained from the upper and lower regions of interfollicular dermal tissue. Small pieces of superficial (papillary) and deep (reticular) dermis were minced, then placed in culture in different 35mm dishes in Dulbecco's Modified Eagle's Medium (DMEM) containing GlutaMAX (Gibco, Invitrogen) supplemented with 20% Fetal Bovine Serum (FBS) (Gibco, Invitrogen), 1% antibiotics-antimycotics (Gibco, Invitrogen). Tissue were maintained at 37°C in a humidified atmosphere of 5% CO<sub>2</sub>/95% air for 10 days, during which time Pfi and Rfi migrated from their respected dermal explants. After migration of fibroblasts outward from the explants, cells were amplified in culture in DMEM GlutaMAX, 10% FBS and 1% antibiotics at 37°C in a humidified atmosphere of 5% CO<sub>2</sub>/95% air, and passaged until p3, at which time they were used to established cell derived ECMs.

Intact dermal papillae were also isolated from the same piece of scalp skin, following a microdissection approach, to obtain DPfi cultures from the same donors as the Pfi and Rfi. Briefly, follicles were transected just above the level of the dermal papilla to isolate

---

end bulbs, which were inverted using 27G needles to remove the matrix and expose the dermal papilla. Papilla were then separated from the follicle by cutting through their stalk. For culture, 6–8 papillae were transferred to 35mm dishes containing 20% FBS in DMEM GlutaMAX, with 1% antibiotics-antimycotics. Cells migrated from the papillae, and when the dish was approaching confluence, DPfi were passaged at a 1:2 ratio using 0.5% trypsin-edta (Gibco, Invitrogen) for detachment. After the initial 2 weeks of culture, cells were grown in DMEM GlutaMAX, 10% FBS and 1% antibiotics. After passaging, DPfi were cultured in the same manner as Pfi and Rfi. Matched sets of cells, from 3 different donors were used for ECM generation and subsequent analysis. For keratinocyte isolation, skin samples were washed briefly in phosphate buffered saline (PBS) containing 2% antibiotics-antimycotics, then incubated in Dispase (Stem Cell Technologies) overnight at 4°C. The epidermis and dermis were then separated from each other with fine forceps. Next, the epidermal layer was minced with scissors, and incubated in 0.5% trypsin-edta at 37°C for 30 minutes. Digested tissue was filtered through a 70µm cell strainer, then cells were pelleted and resuspended in Epilife medium (Gibco, Invitrogen) with 1% antibiotics and EDGS (Gibco, Invitrogen). Cells were grown in a humidified atmosphere of 5% CO<sub>2</sub>/95% air and used for skin construct generation at P2.

### ***3.1.2 ECMs generation***

To generate ECMs from dermal fibroblast sub-populations we followed previously described protocols [58] (Figure 9). Sterile 13 mm glass coverslips in a 24 well-plate were coated with 0.2% sterile gelatin (gelatin type B, Sigma Aldrich) for 60 min at 37°C. They were washed 3 times with PBS, cross-linked with 1% sterile glutaraldehyde (Sigma Aldrich) for 30 min at room temperature (RT) and again washed 3 times with

PBS. Crosslinking was quenched with 1M sterile glycine in PBS for 20 min at RT, followed by 3 more washes in PBS. Coverslips were then incubated in growth medium (DMEM GlutaMAX, 10% FBS, 1% antibiotics) for 30 min at 37°C. Finally, coverslips were washed 3 more times with PBS, then used immediately. The three different sub-populations of fibroblasts (DPfi, Pfi, Rfi) were plated onto coverslips in 24 well plates. A total of 65,000 cells were seeded into each well in DMEM GlutaMAX, 10% FBS, 1% antibiotics and cultured overnight in 37°C, 5% CO<sub>2</sub>/95% air to achieve full confluency. The next day, growth medium supplemented with 50 µg/ml ascorbic acid (Sigma Aldrich) was added to each culture to promote self-assembly of ECM. Medium was exchanged for fresh medium every two days for a total of ten days. After ten days of culture in ascorbic acid supplemented medium, cells were removed. Medium was aspirated and cells were washed once with PBS. Pre-warmed extraction buffer (20mM NH<sub>4</sub>OH, 0.5% Triton X-100 in PBS) was then added and left for 4 min to allow cell lysis. Half of the buffer was carefully removed and PBS was added. The same step was repeated until no intact cells were visible. The DNA residue was digested with 10 µg/ml DNase I (Roche) in PBS for 30 min at 37°C, 5% CO<sub>2</sub>, followed by two washes with PBS.

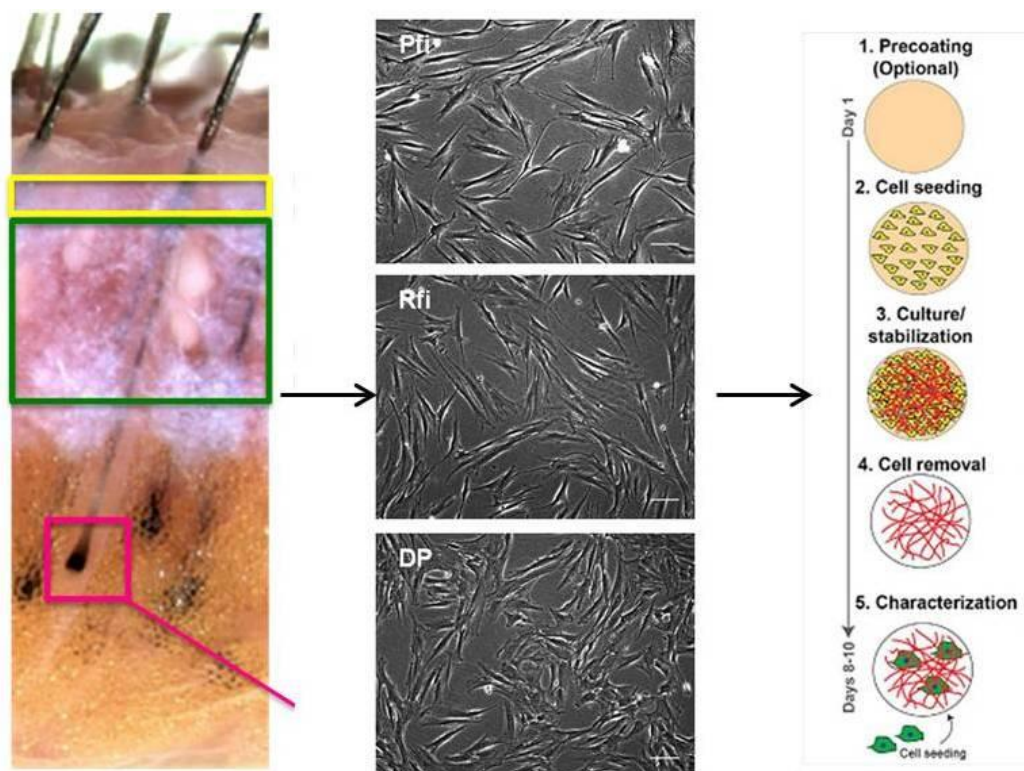


**Figure 9:** Protocol followed to generate ECMs from dermal fibroblast sub-populations.

### 3.1.3 *ECMs analysis*

#### Immunofluorescence staining and analysis of cell assembled ECMs

I performed immunofluorescence of specific proteins in the self-assembled matrices using antibodies against individual ECM components. Matrices were fixed using 4% paraformaldehyde (PFA) for 20 minutes, followed by wash and blocking steps with 5% goat serum (Vector Laboratories) in PBS for 30 minutes. Primary antibodies (Table 1) were diluted in PBS and placed on matrices overnight at 4°C. Secondary antibodies (Table 1) were used for 1 hour at room temperature. Finally, they were washed 3 times in PBS and mounted on glass slides with Vectashield mounting medium (Vector Laboratories).

<b>Antigen</b>	<b>Source</b>	<b>Species (raised in)</b>	<b>Dilution used</b>
<b>FIBRONECTIN</b>	Sigma-Aldrich	Rabbit	1:500
<b>COLLAGEN 1</b>	Abcam	Mouse	1:300
<b>COLLAGEN 6</b>	Abcam	Rabbit	1:500
<b>TENASCIN C</b>	Abcam	Mouse	1:300
<b>THROMBOSPONDIN</b>	Abcam	Mouse	1:50
<b>Anti mouse-ALEXA fluor 488</b>	Molecular Probes	Goat	1:200
<b>Anti rabbit-ALEXA fluor 546</b>	Molecular Probes	Goat	1:200

**Table 1:** Primary and secondary antibodies used for ECMs analysis.

After staining, ECMs were imaged using a Zeiss LSM-510 inverted confocal microscope. Z-stack images of slices were acquired for each fibronectin stained sample, which were used for the evaluation of alignment and fiber measurements. Three random stacks were imaged per coverslip giving a total of nine images per cell donor. Moreover, the thickness of the ECMs was determined by taking a z-stack image on the confocal microscope and subtracting the distance between the top and the bottom of assembled fibronectin matrix. The images were subsequently processed with Image J and Fiji programs. Each z-stack set of images was converted to a single image by using the maximum projection function. The plugin dimensionality was applied to calculate the orientation distribution of the fibres, while the diameter of the fibres and interfibrillar spaces were assessed with the plugin BoneJ [59].

### ECM samples directly analyzed by mass spec

The protocol I used for mass spectrometry was described previously by Plieger et al. [60]. After cell elimination, ECM proteins were directly proteolyzed in each well using 2.5µg trypsin (Gibco, Invitrogen) in 250 µL of 30mM Tris (pH 8.0) at 37°C overnight. Predigested matrix proteins were scraped off from the wells using a cell scraper and collected into 1.5mL microfuge tubes. The samples were then reduced by the addition of DTT (final concentration 10mM) and incubated for 30 min at 56°C. After reduction, Iodoacetadime (IAM, final concentration 55mM) was added to keep the disulfide bonds separate and unfolded, and incubated for 30 min at RT in the dark. Finally, the samples were further digested by trypsin at 37°C overnight before terminating the digest with the addition of 10% trifluoroacetic acid (final concentration 0.5%). Samples were analysed by LC–MS using a nanoAcquity UPLC™ system (Waters MS Technologies, Manchester, UK). 1 µL (1-3 µg protein digest) of sample was injected onto each trapping column (Waters, C18, 180µm×20mm) using partial loop injection, for 1 min at a flow rate of 15µL/min with 0.1% (v/v) formic acid. The sample was resolved on the analytical column (Waters, nanoACQUITY UPLC™ M-class HSS T3 75µm×150mm 1.8µm column) using a gradient of 97% A (0.1% (v/v) formic acid) 3% B (99.9% acetonitrile 0.1% (v/v) formic acid) to 60% A 40% B over 36 min at a flow rate of 300nL/min. The nanoAcquity UPLC™ was coupled to a Synapt™ G2 mass spectrometer (Waters) and data acquired using a MS<sup>E</sup> program with 1s scan times and a collision energy ramp of 15–40eV for elevated energy scans. The mass spectrometer was calibrated before use and throughout the analytical run at 1min intervals using the NanoLockSpray™ source with glufibrinopeptide. Peptide identification was performed by using ProteinLynx Global SERVER™ v3.1

(Waters). The data was processed using a low energy threshold of 150 and an elevated energy threshold of 30. A fixed carbamidomethyl modification for cysteine was specified. The search thresholds used were: minimum fragment ion matches per peptide 3; minimum fragment ion matches per protein 7; minimum peptides per protein 2 and a false positive value of 4. Data was searched against the most recent UniProtKB/Swiss-Prot human database entry [61].

#### ***3.1.4 Generation of epidermal only skin constructs***

For this experiment, I used fibroblasts and keratinocytes as isolated in section 3.1.1. To start I placed several cell inserts (Millicell-24 Cell Culture Insert Plate, polycarbonate, 0.4 $\mu$ m) into a 60mm cell culture dish, and coated using the same method for coverslip coating as described in section 3.1.2. I seeded each fibroblast sub-populations at a density of 30,000 cells/insert in DMEM GlutaMAX, 10% FBS, 1% antibiotics and allowed the fibroblasts to produce ECMs for 10 days in ascorbic acid supplemented medium on the inside of each insert. After removing fibroblasts, I seeded 250,000 keratinocytes inside each insert on the top of the cell depleted ECMs, in Cnt Prime Medium (CellnTec). After 2 days, I removed the Cnt Prime Medium from the inserts and added 3D Barrier Medium (CellnTec) both inside and outside the inserts. The next day all 3D Barrier Medium was removed, and replaced with fresh 3D Barrier Medium on the outside of the inserts only. This enables establishment of an air liquid interface which is required for epithelial stratification. Finally, I kept the cells for 14 days in culture at the air liquid interface, prior to analysis.

### ***3.1.5 Skin constructs analysis: viability and basement membrane formation***

I used an alamar blue assay to assess cell viability of epidermal skin constructs after 14 days of culture. Resazurin, the active ingredient of alamarBlue® reagent (Invitrogen), is reduced upon entering cells to resorufin, a compound that is red in color and highly fluorescent. Viable cells continuously convert resazurin to resorufin, increasing the overall fluorescence and color of the media surrounding cells. Alamar blue dye at a concentration of 10% in PBS was added to each skin construct and incubated for 4 h at 37 °C in 5% CO<sub>2</sub>/95% air. 100 µl of the medium was transferred to a fresh 96 well plate and absorbance was read at 570 nm. Data were expressed as an absorbance value unit.

Alternatively, after the growth period of 14 days at the air-liquid interface, samples were snap-frozen in OCT mounting medium and stored at -80°C until processing. Frozen samples were sectioned into 7µm slides using a cryostat. For staining, these were fixed with either 4% PFA in PBS for 10 min at RT, or 100% methanol for 7 minutes at -20C. After fixation, the samples were rinsed 3x with PBS and pre-treated for 30 min with PBS containing 5% goat serum, followed by incubation overnight at 4°C with primary antibodies (Table 2). The sections were thoroughly rinsed with PBS and then incubated with secondary antibodies for 1hr at RT. Coverslips were mounted using Vectashield containing DAPI (Vector Laboratories), which subsequently labels nuclei. Confocal microscopy (Zeiss LSM-510 inverted) was used to visualize and capture immunostained cells.

Antigen	Source	Species (raised in)	Dilution used
LAMININ 5	R&D systems	Mouse	10 µg/mL
COLLAGEN 7	Abcam	Mouse	1:500
COLLAGEN 4	Abcam	Mouse	1:50
Anti mouse-ALEXA fluor 488	Molecular Probes	Goat	1:200

**Table 2:** Primary and secondary antibodies used for Skin constructs analysis.

For transmission electron microscopy, 14 days old constructs were fixed in 2.5% glutaraldehyde in 0.1 M cacodylate buffer at pH 7.2-7.4, washed in 0.1 M cacodylate buffer at pH 7.2, postfixed in 1% OsO<sub>4</sub> in 0.1 M cacodylate buffer at pH 7.2, dehydrated in graded ethanol and embedded in Araldite (Serva). Ultrathin sections were counterstained with uranyl acetate and lead citrate and examined under a Zeiss EM109 transmission electron microscope to evaluate basement membrane formation within the constructs.

### **3.1.6 Graphs and statistical analysis**

All graphs were generated using GraphPad Prism version 6.01. Data are shown as the mean while error bars ( $\pm$ ) are the standard deviation of the mean. One-way ANOVA followed by Bonferroni's correction was performed for experiments, with  $p < 0.05$  considered significant.

## **3.2 Investigation of Human Decellularized Dermal Matrix (HDM) regenerative ability in the reconstruction of Abdominal Wall Defects**

### ***3.2.1 Tissue procurement***

2-3 mm thick samples of human dermis were first taken from the backs of multi-organ and/or multi-tissue donors and then transported to the RER Skin Bank for processing according to national rules on tissues for transplantation (CNT 14/09/2016); here the tissues were aseptically decellularized and stored in nitrogen vapors (-180°C). At 24 hours before surgical implantation, tissue samples of requested sizes were thawed, prepared and then sent in a sterile saline solution from the RER Skin Bank to Emergency Surgery and Trauma, of Bufalini Hospital and here conserved at a temperature of 4°C until its use.

### ***3.2.2 Patient population and surgical procedure***

Between June 2012 and December 2014, 64 patients, average age 64 years, received human decellularized dermal matrix (HDM) after signing consent forms, to replace and cover the damage area during abdominal wall defects surgery. Abdominal wall reconstruction was performed using the components separation technique by Ramirez et al. [62]. Briefly, this surgical technique is based on subcutaneous lateral dissection, fasciotomy lateral to the rectus abdominis muscle and dissection on the plane between external and internal oblique muscles with medial advancement of the block that includes the rectus muscle and its fascia. This release permits medial advancement of the fascia and a closure up to 20 cm wide defects in the midline area. Then HDM was positioned in a bridge onlay technique in aseptic conditions and then it was sutured

(Figure 10A). Finally, the incision was then dressed with a negative pressure wound therapy dressing (Figure 10B).

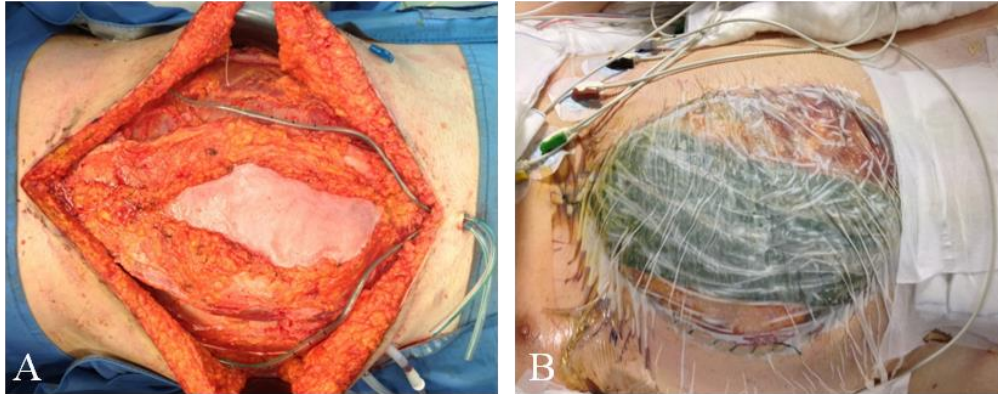


**Figure 10:** Digital photographs illustrating surgical technique used by the surgeons. (A) Bilateral release of the external oblique muscles allowed for a tension-free fascial closure of this large deficit. Then a sheet of decellularized human dermis was placed as an overlay reinforcement and sutured. (B) The incision was finally dressed with a negative pressure wound therapy dressing.

The number and the size of the drains varied based on the size of the overlying skin flaps. In the case of large abdominal wall defects (Figure 11A), multiple pieces of human decellularized matrix were sutured together on the operating table and were inset to the fascial edges (Figure 11B).

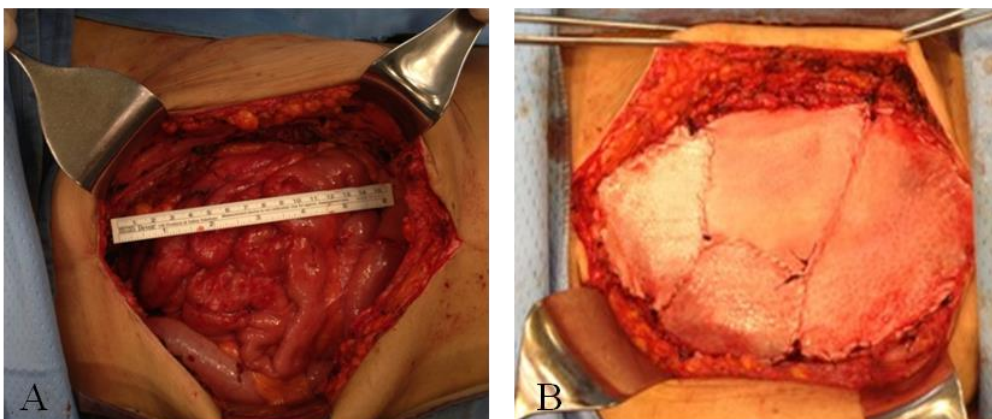


**Figure 11:** Digital photographs illustrating one case with large deficit from the series. (A) Large abdominal wall defects. (B) Multiple pieces of decellularized human dermis were sutured together and were inset to the fascial edges.

After surgical procedures, all patients were followed weekly for the first month and then monthly up to 6 months postoperative and any major problem or complication were recorded. Six months follow up included abdominal exams, serological tests for the potential detection of HBV, HCV and HIV virus and magnetic resonance imaging (MRI) analysis in order to evaluate integration of HDM with the patient's surroundings tissues and eventual long-term complications.

### ***3.2.3 Histological and ultrastructural analysis of HDM biopsy specimens***

#### **Biopsy specimen's collection**

Biopsy specimens were taken after signing consent forms from 3 patients, 1 female and 2 males (average age 60 years), suffering from recurrent hernia at 1 year after the first abdominal wall reconstruction. The initial repair used a 2-3 mm thick HDM taken from the backs of 3 different tissue donors, processed and stored until its use at the RER Skin Bank, following the surgical technique described above. One year later, all the 3 patients developed another hernia in a different abdominal area. During the second surgery, it was evident that the HDM previously transplanted was well incorporated by the surrounding tissues without any sign of inflammation. Thus, biopsy specimens of human decellularized dermis were taken from the previously transplanted area (different parts as transplant mapping).

#### **Histological analysis**

Biopsy specimens were fixed in 10% neutral buffered formalin and embedded in paraffin. Five to seven  $\mu\text{m}$  paraffin sections were stained with hematoxylin and eosin (H&E), Masson's trichrome and Weigert for morphological, collagen and elastic fibers analysis respectively. As control the same unimplanted HDM was prepared and stained following the same protocol. Semiquantitative histometric analysis was performed and

included evaluation of the amount of cellular infiltration, the presence of multinucleated giant cells, new blood vessels formation, the degree of the connective tissue organization. For the histometric analysis, we followed the methods described by *Valentin JE et al., 2006* [63] (Table 3). A pathologist examined all the slides and then assigned scores on four selected fields at the same magnification (40X) for each patient's slide.

Criterion	0	1	2	3
Cellular infiltration	Between 0 and 50 cells per HPF	Between 51 and 100 cells per HPF	Between 101 and 150 cells per HPF	More than 150 cells per HPF
Multinucleated giant cells	No multinucleated giant cells per HPF	Between 1 and 2 multinucleated giant cells per HPF	Between 3 and 4 multinucleated giant cells per HPF	More than 5 multinucleated giant cells per HPF
Vascularity	Either 0 or 1 blood vessel per HPF	Between 2 and 5 blood vessels per HPF	Between 6 and 10 blood vessels per HPF	More than 10 blood vessels per HPF
Connective-tissue organization	Original scaffold intact	Original scaffold disrupted, poorly organized, new host extracellular matrix present	Moderately organized connective tissue present	Dense highly organized connective tissue present

\*HPF= high power field (x40)

**Table 3:** Scoring Criteria of the Semiquantitative Histometric Analysis. At forty times magnification the analysis were based on 4 selected fields/ patient's slide [63].

### Ultrastructural analysis

Biopsy specimen fragments were fixed in 2.5% glutaraldehyde in 0.1 M cacodylate buffer at pH 7.2-7.4, washed in 0.1 M cacodylate buffer at pH 7.2, postfixed in 1% OsO4 in 0.1 M cacodylate buffer at pH 7.2, dehydrated in graded ethanol and embedded in Araldite (Serva). Ultrathin sections were counterstained with uranyl acetate and lead citrate and examined under a Zeiss EM109 transmission electron microscope, to evaluate the ultrastructural dermis organization both at cellular and stromal level.



## 4. RESULTS AND DISCUSSION

---

### 4.1 Differences in fibroblast extracellular matrices (ECMs) and their role in supporting keratinocytes growth and basement membrane formation

In the last two decades, the key role of ECM in cell biology has become more evident. Indeed, ECM is known to regulate cell behaviour, and it plays an essential role during organ development, function and repair [64]. On this basis, ECM as a molecular scaffold is fundamental for tissue homeostasis and alterations in a specific ECM component can lead to disruption of this process [65]. Physical properties such as topography and porosity of ECM can influence various anchorage-related biological functions such as cell division and migration [66]. Given the importance of ECM in cell biology, ECM scaffolds are starting to become commonplace for tissue repair [67]. However, within the skin at least, dermal replacements used to promote regeneration are insufficient. They are composed of only a simple ECM, or decellularized reticular dermis, and they do not take into account the heterogeneity within whole skin dermis [2]. These limitations highlight the need for bioinspired scaffolds for skin repair. ECM scaffolds derived from cultured cells offer several advantages compared with decellularized tissues; there are lower risks of pathogen transmission and undesirable inflammatory and immunological reactions [68].

#### **4.1.1 ECMs thickness and morphology**

I first generated cell assembled matrices from each of the three fibroblast sub-populations; DPfi, Pfi and Rfi. Using confocal microscopy images of FIBRONECTIN (FINC) coupled with image analysis algorithms we found that the composition, morphology and architectural structure of the self-assembled ECMs varied between each of the three fibroblast sub-populations used (Figure 12 A-C). Specifically, Pfi generate matrices with significantly thicker fibres than DPfi and Rfi, which are associated with lowest amount of interfibrillar space between each fiber (Figure 12 D, E). The fact that Pfi generate matrices with significantly thicker fibres than DPfi and Rfi is different to ECM organization *in vivo*, where the papillary dermis contains thinner fibers than the reticular dermis [5]. However, with regards to organization, we observed parallels in our cell assembled ECMs, to ECM in different locations within the skin dermis *in vivo*. In fact, Pfi derived ECM fibers were significantly anisotropic compared to both Rfi and DPfi derived matrices (Figure 12 F). This bears resemblance to the papillary dermis, which is disorganised in comparison to the reticular dermis [5]. Lastly, when we assessed matrix thickness, the DPfi deposited significantly more matrix than both Rfi and Pfi (Figure 12 G). In fact, in the hair follicle a thick basement membrane, termed a glassy membrane, separates the dermal papilla from the surrounding epithelial matrix [69].

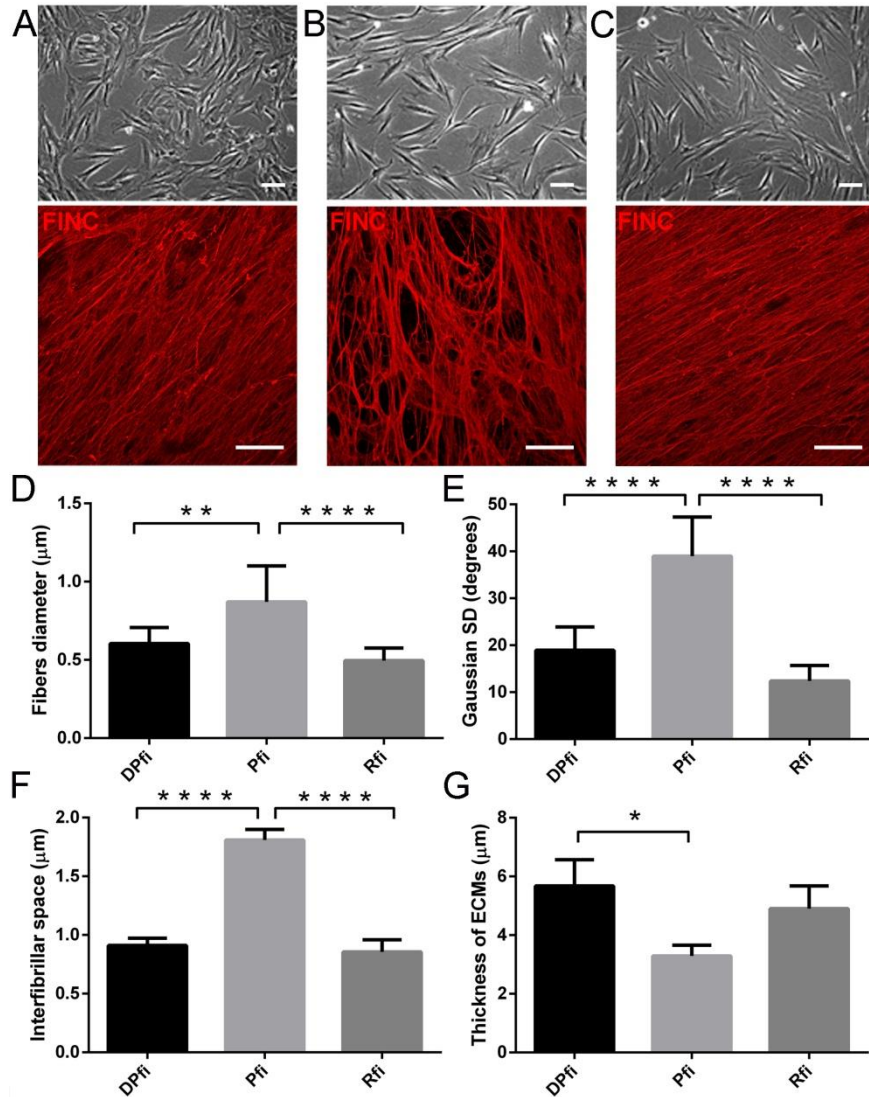


**Figure 12:** Morphological characterisation of cell assembled ECMs. Phase contrast images of cells, and representative immunofluorescence images of FIBRONECTIN (FBN) stained ECMs generated by DPfi (A), Pfi (B) or Rfi (C) after 10 days in culture.

#### 4.1.2 ECMs composition

Given the different fiber morphologies in our cell assembled ECMs from different fibroblast sub-populations, we wanted to determine whether there were differences in matrix composition. To do this, we performed mass spectrometry analysis of digested matrix proteins. The analysis identified different proteins in the range of 800-4000

Dalton. In total, 13 extracellular matrix proteins were identified within the DPfi, Pfi and Rfi cell assembled ECMs (Table 4).

Protein	Protein avgMass	Protein Matched Peptide IntenSum		
		DPfi	Pfi	Rfi
FINC_HUMAN	266217,54	9163420	5802190,8	7403315,84
COL1A1_HUMAN	139968,14	463655,5	--	52381,07
COL1A2_HUMAN	129827,27	219029	--	--
COL6A1_HUMAN	109670,06	1337386	118216	221323,57
COL6A2_HUMAN	109777,13	758071,5	--	--
COL6A3_HUMAN	345380,56	3940456	242998,8	856061,15
TNC_HUMAN	246499,36	1674585,5	876852,2	1101812,47
TSP1_HUMAN	133374,73	475685,8	--	141405,50
VTNC_HUMAN	132332,61	12644,1	--	--
FBLN2_HUMAN	334344,74	147845,5	85106,7	245734,33
VIME_HUMAN	53708,79	123973	--	--
FBN1_HUMAN	332881,9	--	--	299088
EMIL1_HUMAN	107978,8	--	--	46777

**Table 4:** Mass spectrometry data showing proteins detected from different fibroblast cell-assembled ECMs; protein avg mass is the average mass of the protein and peptide intensity sum is a sum of all the peptide fragments for each protein that the machine detected.

Specifically, FIBRONECTIN and TENASCIN (TNC) were produced by all three different fibroblasts subpopulations. Intriguingly, alpha 1 chain COLLAGEN 1 (COL1A1), which is generally thought to be expressed throughout the dermis, was not

detected in Pfi ECM. We found that while alpha 1 chain COLLAGEN 6 (COL6A1) and alpha 3 chain COLLAGEN 6 (COL6A3) were present in all ECMs derived from all cell types, alpha 2 chain COLLAGEN 6 (COL6A2) was predominantly found in the DPfi ECM. TSP1, VITRONECTIN (VTNC), FIBULIN 2 (FBLN 2), VIMENTIN (VIME), FIBRILIN 1 (FBN 1) and EMILIN 1 (EMIL 1) were also only detected in DPfi or Rfi ECM. Interestingly, it's possible to classify the identified proteins, according to the type, in 4 groups: collagens (alpha 1 and 2 chain of COLLAGEN 1 and alpha 1, 2 and 3 chain of COLLAGEN VI); adhesion proteins (FIBRONECTIN and VITRONECTIN); cellular proteins (VIMENTIN) and other ECM proteins (TENASCIN C, THROMBOSPONDIN, FIBULIN 2, EMILIN 1 and FIBRILIN 1). It's worth mentioning the absence of COLLAGEN 3, ELASTIN, glycosaminoglycans (GAG's) and hyaluronic acid (HA), which are usually key components of ECMs [70]. This could be due to limit of detection of the mass spectrometer but also for the relative short time of fibroblasts culture to deposit ECMs. Firstly, the complex overlap between protein spectra makes for difficult analysis: database searches are not perfect at identifying proteins, and in some cases may falsely identify a protein [71]. Instead, in order to support the hypothesis of early ECMs, I want to highlight the presence of fibrilin 1. In fact, the elastic fibers are composed by a central elastin core covered by a sheath of microfibrils, consisting of different glycoproteins including fibrilin 1. During embryonic development, microfibrils appear before elastin and form a scaffold on which elastin is deposited [72]. In addition, to verify that proteins detected in mass spectrometry analysis were expressed within our cell derived ECMS, I stained each cell assembled ECM with antibodies against COL1 (all chains), COL6 (all chains), TNC and TSP1. Despite not finding COL1A1 in our Pfi ECM, COL1 was present in all samples

(Figure 13 A). Likewise, TNC was present at similar levels across all cell derived ECMs (Figure 13 B). The COL6 antibody detected all alpha chains and we found equal expression in all our ECMs (Figure 13 C), however, TSP1 was predominantly expressed in DPfi derived matrix (Figure 13 D). We used image analysis to quantify expression levels, and confirm these observations (Figure 13E-H). These results both confirm our mass spectrometry data, and corroborate previous reports, in which TSP1 was estimated to be more abundant within the dermal papilla, as appose to the interfollicular skin dermis [73].

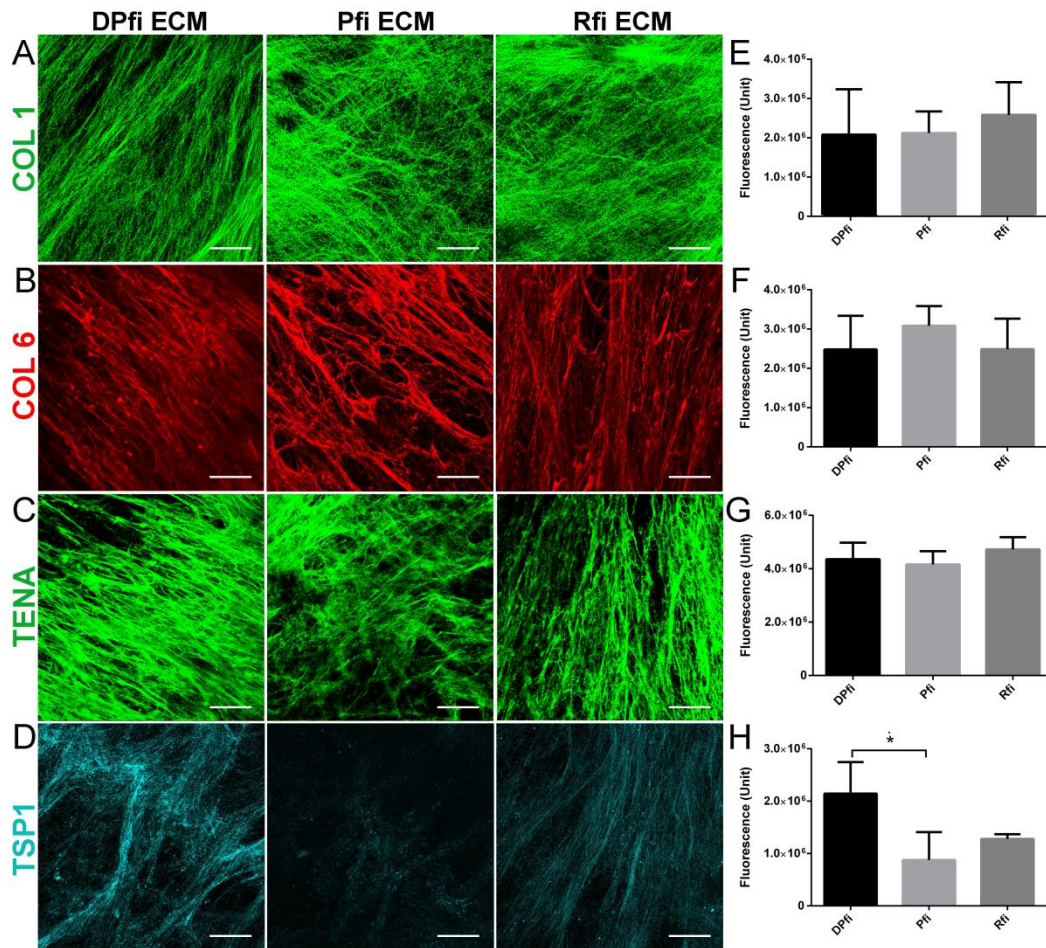


**Figure 13: ECMs composition.** Representative immunofluorescence images of COL1 (A), COL6 (B), TNC (C) and TSP1 (D) in ECMs generated by DPfi, Pfi or Rfi cells after 10 days in ascorbic acid supplemented medium. Quantification of immunofluorescence is plotted in graphs (E-H) (n=3 experiments, 9 images per experiment). \*p<0.05, \*\*p<0.01. Scale bars: 50  $\mu$ m.

To conclude, the composition of cell assembled ECM in vitro is also similar to the ECM in the spatial locations from where the cells were derived. In particular, TSP1 was preferentially deposited by DPfi, while the in vivo dermal papilla is rich in TSP1. The dermal papilla has a critical role in the regulation of hair growth [74], as compared to reticular or papillary dermis [73], which do not express TSP1.

#### 4.1.3 Skin constructs analysis

After determining that ECMs could be successfully generated from each fibroblast subtype, we decided to employ a protocol to generate epithelial only skin constructs, replacing the collagen coating which is usually used with ECM assembled from each cell type. Using alamarBlue to assess keratinocyte viability, we found no significant statistical differences between epithelial only constructs grown on different self-assembled ECMs compared to the control (Figure 14 A).

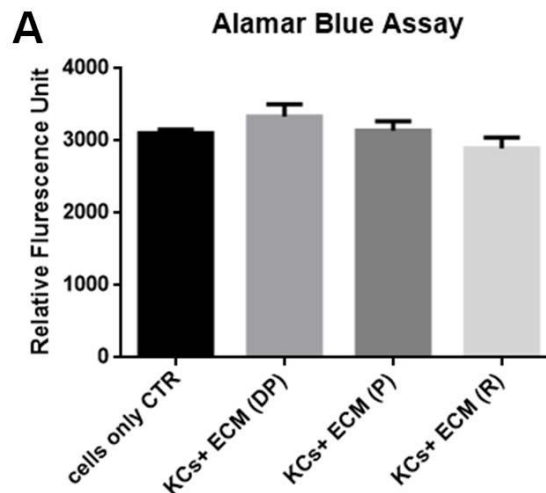


**Figure 14:** Epithelial only skin constructs grown on cell assembled ECMs. (A) Viability assay of cultured keratinocytes on different fibroblast derived matrices (mean  $\pm$  standard deviation).

Next, we specifically wanted to assess basement membrane formation, since our fibroblast sub-populations were derived from sub-anatomical locations subjacent to, and devoid of basement membrane. We used antibodies against LAMININ 5 (LAMA5), COLLAGEN 4 (COL4) and COLLAGEN 7 (COL7) to assess basement membrane characteristics. LAMA5, and COL4, which are deposited from both fibroblasts and keratinocytes [75], were observed only in the constructs grown on Pfi ECM, DPfi ECM and in the control group (Figure 15 and 16 A,B,C). On the contrary, we were unable to find either of these proteins in constructs supported by Rfi (Figure 15 and 16 D).

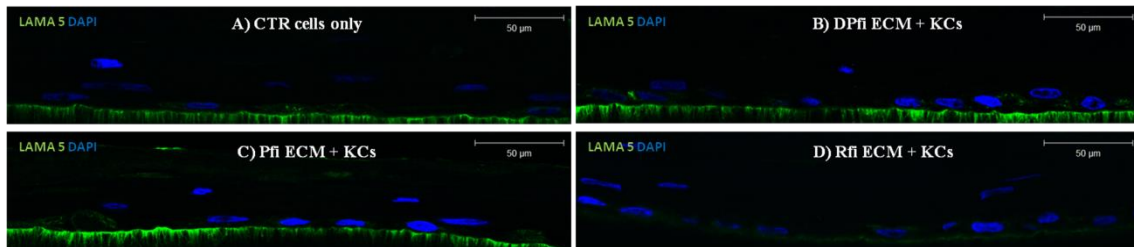


**Figure 15:** Immunofluorescence images of LAMA5 in epithelial only constructs cultured on coating matrix (A), or DPfi (B), Pfi (C) and Rfi (D) derived ECM. (n=3) Scale bars: 50µm.

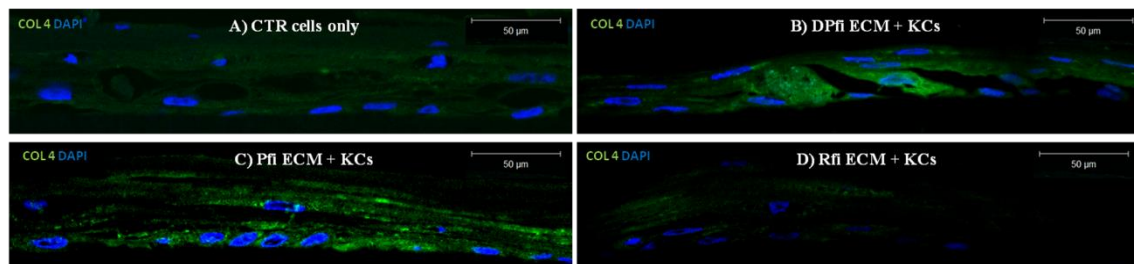


**Figure 16:** Immunofluorescence images of COL4 in epithelial only constructs cultured on coating matrix (A), or DPfi (B), Pfi (C) and Rfi (D) derived ECM. (n=3) Scale bars: 50µm.

COL7, whose production in keratinocytes is stimulated by fibroblasts, was found in both DPfi and Pfi matrix supported constructs (Figure 17 B, C). However, COL 7 was not expressed in the control group (epithelial constructs on coating only), or in the Rfi ECM supported constructs (Figure 17 A, D).

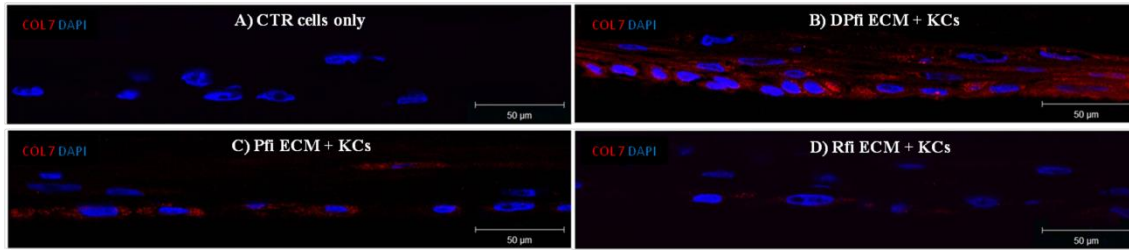


**Figure 17:** Immunofluorescence images of COL7 in epithelial only constructs cultured on coating matrix (A), or DPfi (B), Pfi (C) and Rfi (D) derived ECM. (n=3) Scale bars: 50μm.

This observation is supported by previous studies, where authors not only found more COL7 production and deposition by fibroblasts in comparison to keratinocytes, but also observed that decellularized fibroblast ECM stimulated the production and deposition of COL7 by keratinocytes [76].

In addition to immunofluorescence, we used transmission electron microscopy to assess the basement membrane formation in our epithelial only skin constructs. Basement membranes could be detected in the control group, and in skin supported by Pfi and DPfi matrices, but not Rfi derived matrices. The skin constructs grown on Pfi matrices had a very clear and continuous basal lamina structure compared to the control. In contrast, the skin constructs supported by DPfi derived ECM had a very thick basement membrane; however, this was not continuous across the entire construct (Figure 18 A). Finally, transmission electron microscopy showed that in constructs supported by all three ECM types, numerous desmosomes (Figure 18 B) were linking cells throughout the basal and suprabasal layers of the epidermis suggesting normal differentiation and stratification.

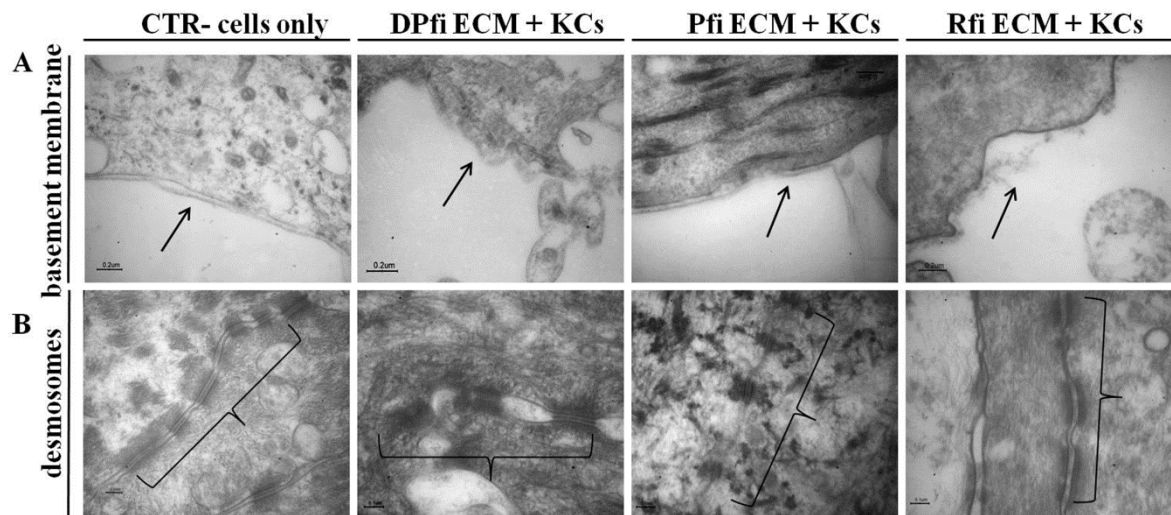


**Figure 18:** Ultrastructural analysis of the basement membrane (arrows) (A) and desmosomes (brace) (B) in the epithelial only skin constructs. (n=3)  
Scale bars for A: 0,2 $\mu$ m and for B: 0,1  $\mu$ m.

It is well known that the skin dermis and its interaction and crosstalk with epithelial cells is important for the production of the basement membrane components [77]. Refocusing on constructs supported by Rfi matrices, I found no evidence of basement membrane establishment with either antibody staining or transmission electron microscopy. This is despite basement membrane formation occurring within our control samples and suggests that there may be an inhibitor of membrane formation within the Rfi matrices [13]. While I removed cells from our matrices, growth factors would remain attached to the ECM. I therefore cannot conclude that this observation is due specifically to the different ECMs, and it is highly likely that the growth factors constituents produced by the different fibroblast sub-types play an important role directing the establishment of a basement membrane [78]. Interestingly, when Pfi and Rfi are grown in co-cultures with keratinocytes, they form cysts [5]. The Rfi-keratinocyte cysts do express LAMA5, however COL7 is absent. This is in contrast to Pfi-keratinocyte cysts which express all basement membrane

components [5]. This again reflects the dermal locations of the cells in vivo, where supporting establishment of a basement membrane is not a part of their repertoire. In contrast, DPfi support establishment of a very thick basement membrane, reflecting their location subjacent to a thickened basement membrane termed a glassy membrane in vivo [69]. It is postulated that the expression of LAMA5 and COL7 in the hair follicle basement membrane is necessary for maintaining the structural integrity of the dermal papilla [13].

## **4.2 Investigation of Human Decellularized Dermal Matrix (HDM) regenerative ability in the reconstruction of Abdominal Wall Defects**

Several studies have demonstrated that human decellularized dermal matrices may achieve excellent results in the treatment of contaminated and complex abdominal wall defects [53]. In fact, it is now well documented that human decellularized matrix has been shown to be associated with lower rates of infection, extrusion, erosion, and adhesion formation compared with synthetic mesh [79]. Specifically, to our knowledge, for the first time a non-commercial decellularized dermis produced by a Skin Bank was implanted to close abdominal wall defects. Moreover, this is the first study of postoperative human biopsy specimens of decellularized human matrix used for hernia repair.

### **4.2.1 Patients clinical follow-up**

A total of 64 patients, 30 females and 34 males, suffering from abdominal wall defects underwent to surgical operation with implantation of decellularized human dermis. Human decellularized dermal matrix was used for patients with different clinical

conditions, such as incisional hernia, Hartmann recanalization, post-traumatic wounds, abdominal tumor, umbilical hernia and rectovaginal fistula. In particular, incisional hernia was the most frequent clinical condition in which HDM was applied, as shown in Table 5, requiring also the highest amount of human decellularized dermis to repair abdominal wall with an average size of 186,5 cm<sup>2</sup>.

<b>Clinical indications</b>	<b>Number of patients</b>	<b>Mean size of decellularized dermis transplanted (cm<sup>2</sup>)</b>
Incisional hernia	40	186,5
Hartmann recanalization	7	76,8
Post-traumatic wounds	6	120
Abdominal tumors	4	125
Umbilical hernia	4	92,2
Rectovaginal fistula	3	52

**Table 5:** Clinical Indications for use of human decellularized dermis, number of patients treated and average size of the tissue graft.

One month after the surgical operation, 61 patients revealed a well tolerability of HDM and a normal wound healing was also identified in all the damage areas. Only 3 patients (4,7%) experienced postoperative infections that were treated with appropriate antibiotic therapy without removal of the HDM. Moreover, the follow up after 6 months reported no signs of dermis rejection and that none of the patients was positive to serological tests, even if the risk of transmitting infectious diseases is extremely low, because of strict human donor control as well as physical and chemical treatments when processing and storing the tissue. Figure 19 depicts the clinical case a 52 years male suffering from incisional hernia (Figure 19 A), that was treated with 3 different sheets of human

decellularized dermis for the reconstruction of abdominal wall, using components separation technique (Figure 19 B). After 1 month, the patient demonstrated a total recovery of the damage area (Figure 19 C) and after 6 months follow-up, MRI analysis demonstrated an intact abdominal cavity with no evidence of hernia and a perfect incorporation of the HDM in the patient surrounding tissues (Figure 19 D). Similar results were also obtained in all patients after MRI analysis, confirming the integration of HDM on the lesion area with the abdominal wall tissues.

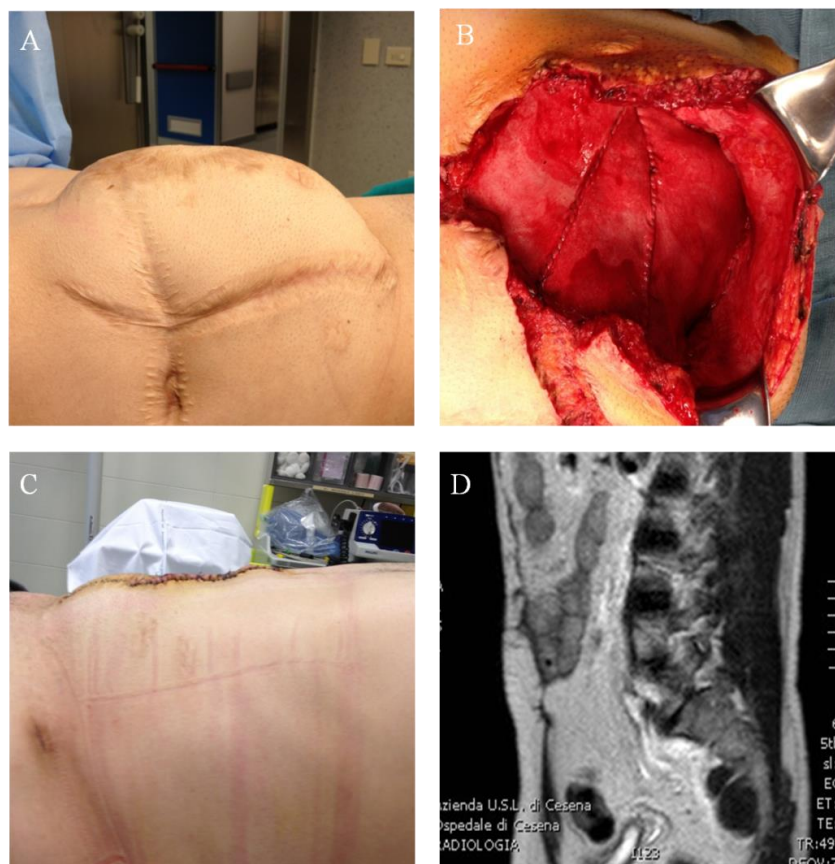


**Figure 19:** (A) Male patient with ventral hernia. (B) Intraoperative view of human decellularized dermis. (C) One month postoperative view of patient following abdominal wall reconstruction. (D) Six-month follow-up using MRI analysis.

Further only few patients developed long term complications such as seroma, as reported in Table 6. Differently from other clinical studies, in which a recurrence hernia frequently occurred, we identified it only in 1 patient. This can be due to the thickness

of our scaffold, which can increase the strength of the tissue graft reducing the recurrence rate. In fact it was suggested that the use of thicker products can prevent stretching of the material over time [80]. Moreover it is worth mentioning the absence of post-implant infections in long-term follow-up, while several studies have demonstrated that animal HDMs could often become infected, resulting in the removal of them [81]. This is due to the fact that this animal tissues are not processed and treated in clean rooms, in compliance with all GMPs standards.

<b>6-months follow-up: results</b>	<b>Number of patients</b>
Perfect integration of the graft with the host tissue	55
Seroma	4
Laxity	3
Recurrence	1
Incisional hernia in a different area	1

**Table 6:** Long-term complications after MRI analysis.

#### ***4.2.2 Histological and ultrastructural findings of HDM biopsy specimens***

##### Light microscopy findings

The HDM pre-transplant was characterized by a dense, acellular, haphazardly structured collagen matrix (Figure 20 A and B), without blood vessels. Moreover, by the use of Weigert staining, numerous randomly disposed elastic fibers were identified (Figure 20 C), which appeared disrupted, likely due to decellularization process. After one year, the HDM biopsy specimens showed numerous fibroblasts and an extensive neoangiogenesis (Figure 20 D in the middle). The graft presented highly oriented

collagen pattern as in a normal dermal tissue (Figure 20 E). The elastic fibers were thin and parallel to collagen fibers (Figure 20 F).

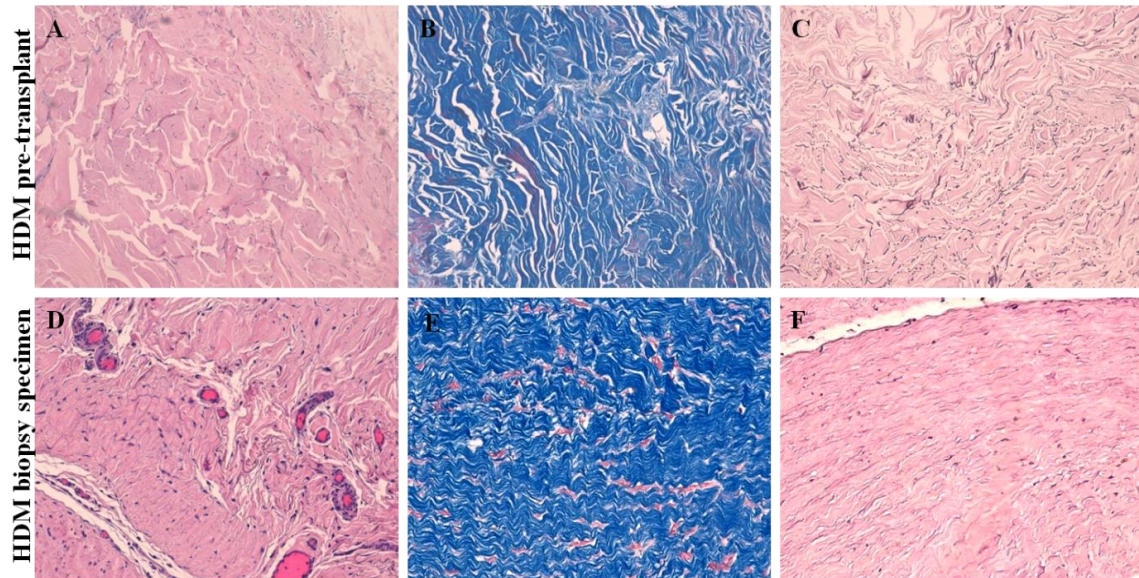


**Figure 20:** Histological comparison between pre-transplant and biopsy specimen HDM. The HDM pre-transplant was decellularized (A) (H&E staining, 10x), characterized by haphazardly structured collagenous fibers (B) (Masson Trichrome staining, 10x) and by numerous disrupted elastic fibers (C) (Weigert staining, 10x). The HDM biopsy specimens showed extensive fibroblast infiltration with numerous new blood vessels (D) (H&E staining, 10x), highly oriented collagen pattern (E) (Masson Trichrome staining, 20x) and thin elastic fibers parallel to collagen fibers (F) (Weigert staining, 20x).

Hypertrophic fibroblasts were present in a small area where the collagen matrix was still in remodeling, as a sign of tissue regeneration (Figure 21 A). Only few inflammatory cells were present at the periphery of the HDM biopsy specimens. Only in patient 2, a typical foreign-body tissue response was present, including few multinucleated giant cells around blood vessels (Figure 21 B).

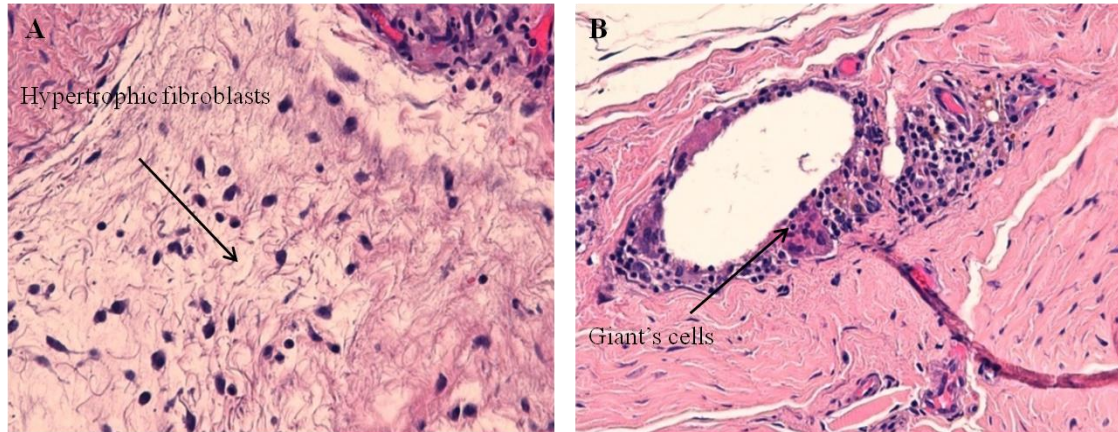


**Figure 21:** H&E stainings HDM biopsy specimen of patient 2, 20X. Hypertrophic fibroblasts (arrow) in a small area where the collagen matrix was still in remodeling (A). A multinucleated Giant's cell (arrow) around blood vessels as a typical foreign-body tissue response (B).

In addition, a histological comparison of HDMs pre-transplant (taken from 3 different tissue donors) was also performed in order to compare the matrix differences before transplant (Figure 22 A, B, C). All the HDMs pre-transplant were well decellularized, but the HDM of donor 2 appeared to be less dense compared to the others two (Figure 22 B).

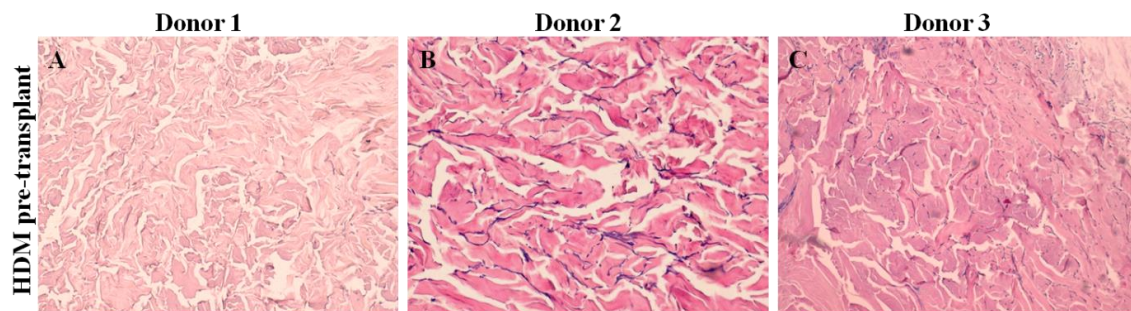


**Figure 22:** Histological comparison between pre-transplant HDM in donor 1 (A), 2 (B) and 3 (C) respectively. (H&E staining, 10x). The HDM pre-transplant were decellularized, characterized by haphazardly structured collagenous fibers. The HDM of donor 2 appeared to be less dense compared to the others two.

### Morphometric analysis findings

The mean scores for the three patients are presented in Table 7. The patient 2 showed the most intense immune response, as assessed by the presence of inflammatory cells

and multinucleated giant cells at the implant site. Blood vessels were also detected in all the implants, while the patient 3 revealed the best connective tissue organization. Taking into account the HDM pre-implant characteristics (Figure 22), a relationship between inflammatory cells and collagen remodeling seemed to be; indeed, the more inflammatory infiltrate was abundant, the organization of connective tissue resulted more improved.

	Cellularity	Multinucleated giant cells	Vascularity	Connective tissue organization
<b>PATIENT 1</b>				
slide 1	0	0	1	3
slide 2	0	0	2	2
slide 3	0	0	1	2
slide 4	0	0	2	3
<b>PATIENT 2</b>				
slide 1	0	0	2	2
slide 2	1	1	2	3
slide 3	1	2	3	2
slide 4	0	0	2	2
slide 5	0	3	2	2
slide 6	0	0	3	3
slide 7	1	1	3	2
<b>PATIENT 3</b>				
slide 1	1	0	3	3
slide 2	0	0	2	3
slide 3	0	0	2	3
slide 4	0	0	2	3
slide 5	1	0	2	3

**Table 7:** Semiquantitative Morphometric Analysis. Mean scores for each patient's slide (four fields at 40x magnification analyzed). The scores for each implant were tabulated according to the criteria in table 6.

### Ultrastructural findings

TEM analysis confirmed histological data. In particular, fibroblast cells showed typical elongated shape with normal nuclei (Figure 23 A): few collagen fibers were seen in the fibroblast cytoplasm suggesting their active synthesis (Figure 23 B). Collagen fibers were characterized by a normal morphology and band size (Figure 23 C). The vascular

structures lined by endothelial cells and smooth muscle cells showed normal morphology (Figure 23 D).

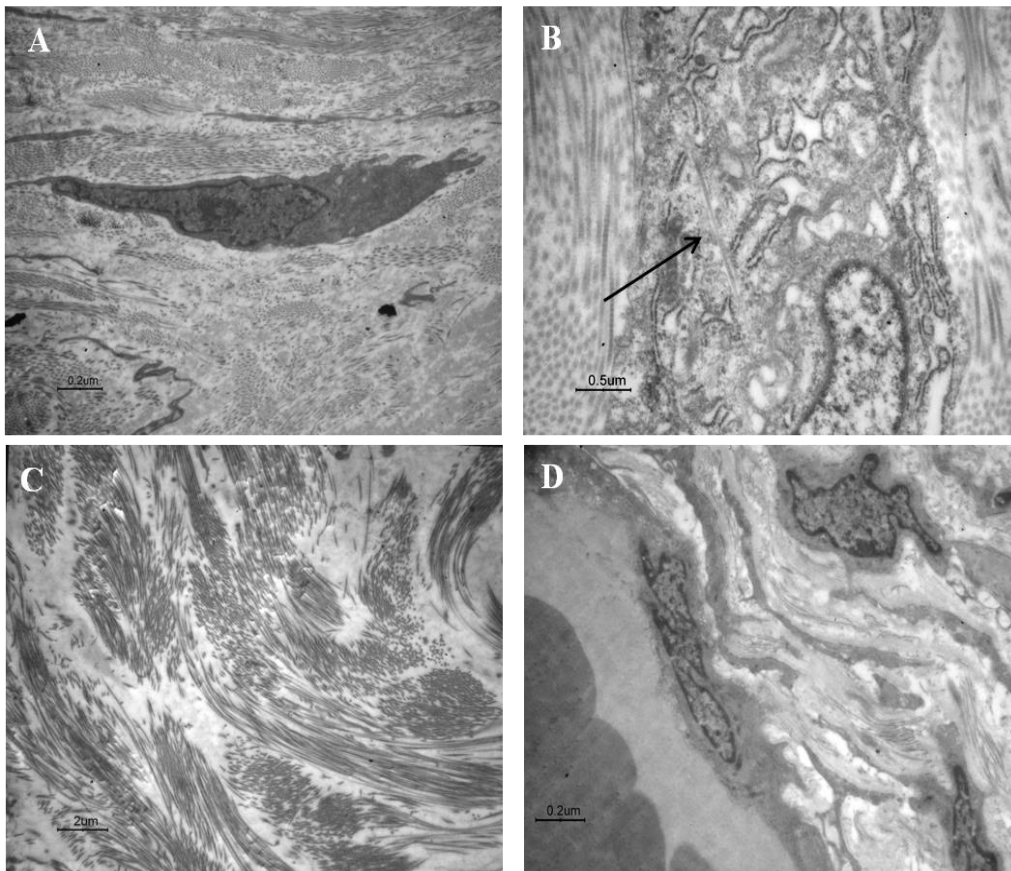


**Figure 23:** Ultrastructural analysis of HDM biopsy specimens: long-shaped fibroblasts (A) (scale bar 0,2 $\mu$ m) producing a collagen fiber (arrow) (B) (scale bar 0,5  $\mu$ m) and normal morphology of collagenous structure (C) (scale bar 2  $\mu$ m); finally, a normal blood vessel (D) (scale bar 0,2  $\mu$ m).

The histological and ultrastructural results from this study support previous preclinical conclusions concerning the HDM produced by RER Skin Bank reported by *Bondioli et al.* [36]. Overall, the RER Skin Bank HDM, transplanted in patients suffering from abdominal hernia, was characterized by cellular repopulation, neoangiogenesis, minimal inflammatory response and a well-organized collagen matrix in all biopsy specimens investigated. In particular, it is well known that natural collagen remodeling is performed through the coordinated enzymatic actions of assorted matrix

metalloproteinases (MMPs) [82]. The minimal inflammation is very important, because host immune cells rapidly infiltrate the graft and facilitate the degradation and the remodeling of HDM [83]. Moreover, it is worth mentioning the correlation between the morphology of HDM pre-implant related to donor age, the inflammatory response and the connective tissue remodeling after one year. These findings showed that the HDM owns pivotal still undefined biologic factors, activating the tissue regeneration process. It has been reported that the degradation products of extracellular matrix (ECM) have a key-role in tissue regeneration, likely due to their chemoattractive effect on endothelial cells, bone marrow derived cells and mesenchymal stem-cells [84]. In addition, HDM bioactivity is also confirmed by growth factors maintenance in the acellular ECM, which are responsible for cell recruitment, proliferation, angiogenesis and tissue regeneration [85]. Considering the criteria for a functional implant [41], it is evident that the HDM can be considered a promising biomaterial for hernia repair representing an inductive template for remodeling with host tissue.



## 5. CONCLUSIONS

---

This PhD thesis deals with the very important issue of the extracellular matrices (ECMs) in the field of skin tissue engineering. Considering the great interest towards ECM to better understand fundamental tissue processes, several tissue-culture models have been developed to study the interplay between its biochemical and biophysical properties, and to understand the molecular origins of cellular behaviors regulated by ECM ligation [18]. For instance, synthetic matrices have been developed with well defined fibers organization and stiffness, using biomaterials as polyethylene glycol (PEG) hydrogels [86]. Although these matrices can be covalently modified with ECM ligands and growth factors [87], they do not resemble to the organizational features of native collagen and often their pore sizes strongly impede cell migration. To overcome this issue, biomaterial specialists have created decellularized ECM scaffold from various tissues, but in particular for those deriving from animal tissues there might be problems associated with inflammation and rejection [88]. For these reasons, scientists investigated new strategies based on in vitro organogenesis approaches [67]. ECM produced by cells, via a self-assembly approach, has been shown to act as a key cell adhesion site and a mechanically strong scaffold free support for tissue engineering [89].

In the first part, I proposed a new approach to produce ECMs based on the concept of organogenesis, starting from different fibroblast subpopulations within the skin dermis. I kept fibroblasts in long term culture with appropriate growth factors to produce a tissue substitute rich in ECM and then after the ECMs characterization, I created epithelial only skin constructs. The results showed that the composition, fiber morphology, and behavior between the different cell derived ECMs varied between each of the three fibroblast sub-populations used. These differences, I observed, reflect differences that are physiologically present between the papillary, reticular, and hair follicle dermis within the skin [5]. The cell-assembly approach might also be used to establish ECM of different thicknesses and strengths, keeping for longer time cells in culture and adding different growth factors [90]. Moreover, I also demonstrated that matrices derived from both DPfi or Pfi could be superior to Rfi derived dermis as an effective product for skin engineering. In fact, Pfi and DPfi support establishment of a well formed basement membrane, reflecting their location subjacent to a thick basement membrane in vivo [91]. I believe that inspiration can be taken from these physiologically different cell-derived ECMs, to improve the design of reliable biomimetic materials with therapeutic potential for skin tissue engineering.

In the second part, indeed, I presented the excellent results obtained after the clinical application of HDM in patients suffering from abdominal hernia. Several clinically approved decellularized matrices are regularly applied in vivo, primarily as tissue fillers with safe outcomes [92]. However, there are studies which reported negative clinical results with some of these commercial products. For instance, it has been shown that porcine small intestinal submucosa (SIS) is associated with complications after implantation. In general these complications included lack of tissue

repopulation and blood vessel infiltration, with high levels of fibrosis in the periphery of the implanted material [93]. In this respect, despite numerous clinical experiences, mechanisms of biomaterial integration with human tissues, and rejection responses in some cases, remain unexplained and poorly dissected. Conversely, the HDM produced by RER Skin Bank not only provided excellent clinical outcomes in the long-term follow up, but also biopsy specimens post-implant showed that HDM has adequate properties to regenerate into functional tissues. I think one of the key features is that it has human origin. Then a careful screening of cadaveric donors is required by National Center for Tissue Transplantation, in order to avoid transmission of infectious diseases. Moreover this tissue is submitted to an ideal decellularization process, which can remove all cellular components, while maintaining natural ECM structure and composition [36]. The result is a perfect integration with the surrounding without any sign of rejection and fibrosis in the periphery of the implanted material. Finally compared to commercial products HDM hasn't a high cost, since it derives from human donation. To conclude this second part showed an effective HDM product in the field of soft tissue repair, adding also relevant data that can serve as reference to establish new decellularized biomaterials technologies.



## 6. REFERENCES

---

- [1] C.L. Simpson, D.M. Patel, K.J. Green, Deconstructing the skin: cytoarchitectural determinants of epidermal morphogenesis, *Nat Rev Mol Cell Biol* 12(9) (2011) 565-80.
- [2] G. Sriram, P.L. Bigliardi, M. Bigliardi-Qi, Fibroblast heterogeneity and its implications for engineering organotypic skin models in vitro, *Eur J Cell Biol* 94(11) (2015) 483-512.
- [3] M. Visscher, M. Robinson, R. Wickett, Stratum corneum free amino acids following barrier perturbation and repair, *Int J Cosmet Sci* 33(1) (2011) 80-9.
- [4] R.A. Harper, G. Grove, Human skin fibroblasts derived from papillary and reticular dermis: differences in growth potential in vitro, *Science* 204(4392) (1979) 526-7.
- [5] J.M. Sorrell, A.I. Caplan, Fibroblast heterogeneity: more than skin deep, *J Cell Sci* 117(Pt 5) (2004) 667-75.
- [6] R.R. Driskell, B.M. Lichtenberger, E. Hoste, K. Kretzschmar, B.D. Simons, M. Charalambous, S.R. Ferron, Y. Heralut, G. Pavlovic, A.C. Ferguson-Smith, F.M. Watt, Distinct fibroblast lineages determine dermal architecture in skin development and repair, *Nature* 504(7479) (2013) 277-81.
- [7] C.A. Jahoda, A.J. Reynolds, Hair follicle dermal sheath cells: unsung participants in wound healing, *Lancet* 358(9291) (2001) 1445-8.
- [8] R. Sennett, M. Rendl, Mesenchymal-epithelial interactions during hair follicle morphogenesis and cycling, *Semin Cell Dev Biol* 23(8) (2012) 917-27.
- [9] R.R. Driskell, F.M. Watt, Understanding fibroblast heterogeneity in the skin, *Trends Cell Biol* 25(2) (2015) 92-9.
- [10] D.R. Zimmermann, M.T. Dours-Zimmermann, M. Schubert, L. Bruckner-Tuderman, Versican is expressed in the proliferating zone in the epidermis and in association with the elastic network of the dermis, *J Cell Biol* 124(5) (1994) 817-25.
- [11] V.A. Lightner, F. Gumkowski, D.D. Bigner, H.P. Erickson, Tenascin/hexabrachion in human skin: biochemical identification and localization by light and electron microscopy, *J Cell Biol* 108(6) (1989) 2483-93.
-

- [12] C. Walchli, M. Koch, M. Chiquet, B.F. Odermatt, B. Trueb, Tissue-specific expression of the fibril-associated collagens XII and XIV, *J Cell Sci* 107 ( Pt 2) (1994) 669-81.
- [13] A.G. Messenger, K. Elliott, G.E. Westgate, W.T. Gibson, Distribution of extracellular matrix molecules in human hair follicles, *Ann N Y Acad Sci* 642 (1991) 253-62.
- [14] M. Tello, C. Spenle, J. Hemmerle, L. Mercier, R. Fabre, G. Allio, P. Simon-Assmann, J.G. Goetz, Generating and characterizing the mechanical properties of cell-derived matrices using atomic force microscopy, *Methods* 94 (2016) 85-100.
- [15] H. Jarvelainen, A. Sainio, M. Koulu, T.N. Wight, R. Penttinen, Extracellular matrix molecules: potential targets in pharmacotherapy, *Pharmacol Rev* 61(2) (2009) 198-223.
- [16] L.E. Tracy, R.A. Minasian, E.J. Caterson, Extracellular Matrix and Dermal Fibroblast Function in the Healing Wound, *Adv Wound Care (New Rochelle)* 5(3) (2016) 119-136.
- [17] G.D. Weinstein, R.J. Boucek, Collagen and elastin of human dermis, *J Invest Dermatol* 35 (1960) 227-9.
- [18] C. Frantz, K.M. Stewart, V.M. Weaver, The extracellular matrix at a glance, *J Cell Sci* 123(Pt 24) (2010) 4195-200.
- [19] D.A. Carrino, J.M. Sorrell, A.I. Caplan, Age-related changes in the proteoglycans of human skin, *Arch Biochem Biophys* 373(1) (2000) 91-101.
- [20] P. Bornstein, E.H. Sage, Matricellular proteins: extracellular modulators of cell function, *Curr Opin Cell Biol* 14(5) (2002) 608-16.
- [21] F. Lin, X.D. Ren, Z. Pan, L. Macri, W.X. Zong, M.G. Tonnesen, M. Rafailovich, D. Bar-Sagi, R.A. Clark, Fibronectin growth factor-binding domains are required for fibroblast survival, *J Invest Dermatol* 131(1) (2011) 84-98.
- [22] M. Xue, C.J. Jackson, Extracellular Matrix Reorganization During Wound Healing and Its Impact on Abnormal Scarring, *Adv Wound Care (New Rochelle)* 4(3) (2015) 119-136.
- [23] M.F. Brizzi, G. Tarone, P. Defilippi, Extracellular matrix, integrins, and growth factors as tailors of the stem cell niche, *Curr Opin Cell Biol* 24(5) (2012) 645-51.
- [24] A.J. Singer, R.A. Clark, Cutaneous wound healing, *N Engl J Med* 341(10) (1999) 738-46.

- [25] H.P. Ehrlich, T.M. Krummel, Regulation of wound healing from a connective tissue perspective, *Wound Repair Regen* 4(2) (1996) 203-10.
- [26] H. Koyama, E.W. Raines, K.E. Bornfeldt, J.M. Roberts, R. Ross, Fibrillar collagen inhibits arterial smooth muscle proliferation through regulation of Cdk2 inhibitors, *Cell* 87(6) (1996) 1069-78.
- [27] S. Ohba, F. Yano, U.-i. Chung, Tissue engineering of bone and cartilage, *IBMS BoneKEy* 6(11) (2009) 405-419.
- [28] E. Catalano, A. Cochis, E. Varoni, L. Rimondini, B. Azzimonti, Tissue-engineered skin substitutes: an overview, *J Artif Organs* 16(4) (2013) 397-403.
- [29] F. Gottrup, J. Apelqvist, P. Price, Outcomes in controlled and comparative studies on non-healing wounds: recommendations to improve the quality of evidence in wound management, *J Wound Care* 19(6) (2010) 237-68.
- [30] C.A. Higgins, M. Roger, R. Hill, A.S. Ali-Khan, J. Garlick, A.M. Christiano, C.A. Jahoda, Multifaceted role of hair follicle dermal cells in bioengineered skins, *Br J Dermatol* (2016).
- [31] J.M. Felder, 3rd, S.S. Goyal, C.E. Attinger, A systematic review of skin substitutes for foot ulcers, *Plast Reconstr Surg* 130(1) (2012) 145-64.
- [32] A.D. Metcalfe, M.W. Ferguson, Tissue engineering of replacement skin: the crossroads of biomaterials, wound healing, embryonic development, stem cells and regeneration, *J R Soc Interface* 4(14) (2007) 413-37.
- [33] D.Q. Nguyen, W.A. Dickson, A review of the use of a dermal skin substitute in burns care, *J Wound Care* 15(8) (2006) 373-6.
- [34] E. Dantzer, F.M. Braye, Reconstructive surgery using an artificial dermis (Integra): results with 39 grafts, *Br J Plast Surg* 54(8) (2001) 659-64.
- [35] A.S. Halim, T.L. Khoo, S.J. Mohd Yussof, Biologic and synthetic skin substitutes: An overview, *Indian J Plast Surg* 43(Suppl) (2010) S23-8.
- [36] E. Bondioli, M. Fini, F. Veronesi, G. Giavaresi, M. Tschon, G. Cenacchi, S. Cerasoli, R. Giardino, D. Melandri, Development and evaluation of a decellularized membrane from human dermis, *J Tissue Eng Regen Med* 8(4) (2014) 325-36.
- [37] B.N. Brown, C.A. Barnes, R.T. Kasick, R. Michel, T.W. Gilbert, D. Beer-Stolz, D.G. Castner, B.D. Ratner, S.F. Badylak, Surface characterization of extracellular matrix scaffolds, *Biomaterials* 31(3) (2010) 428-37.

- [38] J.A. Soler, S. Gidwani, M.J. Curtis, Early complications from the use of porcine dermal collagen implants (Permacol) as bridging constructs in the repair of massive rotator cuff tears. A report of 4 cases, *Acta Orthop Belg* 73(4) (2007) 432-6.
- [39] R. Rotini, A. Marinelli, E. Guerra, G. Bettelli, A. Castagna, M. Fini, E. Bondioli, M. Busacca, Human dermal matrix scaffold augmentation for large and massive rotator cuff repairs: preliminary clinical and MRI results at 1-year follow-up, *Musculoskelet Surg* 95 Suppl 1 (2011) S13-23.
- [40] J.L. Bond, R.M. Dopirak, J. Higgins, J. Burns, S.J. Snyder, Arthroscopic replacement of massive, irreparable rotator cuff tears using a GraftJacket allograft: technique and preliminary results, *Arthroscopy* 24(4) (2008) 403-409 e1.
- [41] S.J. Snyder, S.P. Arnoczky, J.L. Bond, R. Dopirak, Histologic evaluation of a biopsy specimen obtained 3 months after rotator cuff augmentation with GraftJacket Matrix, *Arthroscopy* 25(3) (2009) 329-33.
- [42] D.K. Lee, A preliminary study on the effects of acellular tissue graft augmentation in acute Achilles tendon ruptures, *J Foot Ankle Surg* 47(1) (2008) 8-12.
- [43] S. Wallace, Histomorphometric and 3D Cone-Beam Computerized Tomographic Evaluation of Socket Preservation in Molar Extraction Sites Using Human Particulate Mineralized Cancellous Allograft Bone With a Porcine Collagen Xenograft Barrier: A Case Series, *J Oral Implantol* 41(3) (2015) 291-7.
- [44] K.S. Al-Hamdan, Esthetic soft tissue ridge augmentation around dental implant: Case report, *Saudi Dent J* 23(4) (2011) 205-9.
- [45] C.L. Winters, S.A. Brigido, B.A. Liden, M. Simmons, J.F. Hartman, M.L. Wright, A multicenter study involving the use of a human acellular dermal regenerative tissue matrix for the treatment of diabetic lower extremity wounds, *Adv Skin Wound Care* 21(8) (2008) 375-81.
- [46] S.G. Chen, Y.S. Tzeng, C.H. Wang, Treatment of severe burn with DermACELL((R)), an acellular dermal matrix, *Int J Burns Trauma* 2(2) (2012) 105-9.
- [47] S.M. Maurice, D.A. Skeete, Use of human acellular dermal matrix for abdominal wall reconstructions, *Am J Surg* 197(1) (2009) 35-42.
- [48] D.J. Leaper, A.V. Pollock, M. Evans, Abdominal wound closure: a trial of nylon, polyglycolic acid and steel sutures, *Br J Surg* 64(8) (1977) 603-6.

- [49] F.C. Usher, The repair of incisional and inguinal hernias, *Surg Gynecol Obstet* 131(3) (1970) 525-30.
- [50] G.J. Lesnick, A.M. Davids, Repair of surgical abdominal wall defect with a pedicled musculofascial flap, *Ann Surg* 137(4) (1953) 569-72.
- [51] J.B. Mulliken, J.K. Wu, B.L. Padwa, Repair of bilateral cleft lip: review, revisions, and reflections, *J Craniofac Surg* 14(5) (2003) 609-20.
- [52] D.M. Parker, P.J. Armstrong, J.D. Frizzi, J.H. North, Jr., Porcine dermal collagen (Permacol) for abdominal wall reconstruction, *Curr Surg* 63(4) (2006) 255-8.
- [53] B. Buinewicz, B. Rosen, Acellular cadaveric dermis (AlloDerm): a new alternative for abdominal hernia repair, *Ann Plast Surg* 52(2) (2004) 188-94.
- [54] G.E. Leber, J.L. Garb, A.I. Alexander, W.P. Reed, Long-term complications associated with prosthetic repair of incisional hernias, *Arch Surg* 133(4) (1998) 378-82.
- [55] A. Aurora, J. McCarron, J.P. Iannotti, K. Derwin, Commercially available extracellular matrix materials for rotator cuff repairs: state of the art and future trends, *J Shoulder Elbow Surg* 16(5 Suppl) (2007) S171-8.
- [56] E.I. Lee, C.J. Chike-Obi, P. Gonzalez, R. Garza, M. Leong, A. Subramanian, J. Bullocks, S.S. Awad, Abdominal wall repair using human acellular dermal matrix: a follow-up study, *Am J Surg* 198(5) (2009) 650-7.
- [57] L.H. Holton, 3rd, D. Kim, R.P. Silverman, E.D. Rodriguez, N. Singh, N.H. Goldberg, Human acellular dermal matrix for repair of abdominal wall defects: review of clinical experience and experimental data, *J Long Term Eff Med Implants* 15(5) (2005) 547-58.
- [58] G. Theocharidis, Z. Drymoussi, A.P. Kao, A.H. Barber, D.A. Lee, K.M. Braun, J.T. Connelly, Type VI Collagen Regulates Dermal Matrix Assembly and Fibroblast Motility, *J Invest Dermatol* 136(1) (2016) 74-83.
- [59] M. Doube, M.M. Klosowski, I. Arganda-Carreras, F.P. Cordelieres, R.P. Dougherty, J.S. Jackson, B. Schmid, J.R. Hutchinson, S.J. Shefelbine, BoneJ: Free and extensible bone image analysis in ImageJ, *Bone* 47(6) (2010) 1076-9.
- [60] D. Pflieger, S. Chabane, O. Gaillard, B.A. Bernard, P. Ducoroy, J. Rossier, J. Vinh, Comparative proteomic analysis of extracellular matrix proteins secreted by two types of skin fibroblasts, *Proteomics* 6(21) (2006) 5868-79.

- [61] E. Boutet, D. Lieberherr, M. Tognolli, M. Schneider, P. Bansal, A.J. Bridge, S. Poux, L. Bougueleret, I. Xenarios, UniProtKB/Swiss-Prot, the Manually Annotated Section of the UniProt KnowledgeBase: How to Use the Entry View, *Methods Mol Biol* 1374 (2016) 23-54.
- [62] L. Heller, C.H. McNichols, O.M. Ramirez, Component separations, *Semin Plast Surg* 26(1) (2012) 25-8.
- [63] J.E. Valentin, J.S. Badylak, G.P. McCabe, S.F. Badylak, Extracellular matrix bioscaffolds for orthopaedic applications. A comparative histologic study, *J Bone Joint Surg Am* 88(12) (2006) 2673-86.
- [64] R.O. Hynes, The extracellular matrix: not just pretty fibrils, *Science* 326(5957) (2009) 1216-9.
- [65] P. Lu, K. Takai, V.M. Weaver, Z. Werb, Extracellular matrix degradation and remodeling in development and disease, *Cold Spring Harb Perspect Biol* 3(12) (2011).
- [66] F. Gattazzo, A. Urciuolo, P. Bonaldo, Extracellular matrix: a dynamic microenvironment for stem cell niche, *Biochim Biophys Acta* 1840(8) (2014) 2506-19.
- [67] P. Kumar, A. Satyam, D. Cigognini, A. Pandit, D.I. Zeugolis, Low oxygen tension and macromolecular crowding accelerate extracellular matrix deposition in human corneal fibroblast culture, *J Tissue Eng Regen Med* (2016).
- [68] H. Lu, T. Hoshiba, N. Kawazoe, I. Koda, M. Song, G. Chen, Cultured cell-derived extracellular matrix scaffolds for tissue engineering, *Biomaterials* 32(36) (2011) 9658-66.
- [69] C.A. Jahoda, Induction of follicle formation and hair growth by vibrissa dermal papillae implanted into rat ear wounds: vibrissa-type fibres are specified, *Development* 115(4) (1992) 1103-9.
- [70] L.M. Mikesch, L.R. Aramadhaka, C. Moskaluk, P. Zigrino, C. Mauch, J.W. Fox, Proteomic anatomy of human skin, *J Proteomics* 84 (2013) 190-200.
- [71] A.I. Nesvizhskii, A survey of computational methods and error rate estimation procedures for peptide and protein identification in shotgun proteomics, *J Proteomics* 73(11) (2010) 2092-123.
- [72] W.F. Daamen, J.H. Veerkamp, J.C. van Hest, T.H. van Kuppevelt, Elastin as a biomaterial for tissue engineering, *Biomaterials* 28(30) (2007) 4378-98.

- [73] J.L. Pablos, E.T. Everett, E.C. Leroy, J.S. Norris, Thrombospondin 1 is expressed by mesenchymal cells in mouse post-natal skin and hair follicle development, *Histochem J* 30(7) (1998) 461-5.
- [74] K. Yano, L.F. Brown, J. Lawler, T. Miyakawa, M. Detmar, Thrombospondin-1 plays a critical role in the induction of hair follicle involution and vascular regression during the catagen phase, *J Invest Dermatol* 120(1) (2003) 14-9.
- [75] M.P. Marinkovich, P. Verrando, D.R. Keene, G. Meneguzzi, G.P. Lunstrum, J.P. Ortonne, R.E. Burgeson, Basement membrane proteins kalinin and nicein are structurally and immunologically identical, *Lab Invest* 69(3) (1993) 295-9.
- [76] P. Benny, C. Badowski, E.B. Lane, M. Raghunath, Making more matrix: enhancing the deposition of dermal-epidermal junction components in vitro and accelerating organotypic skin culture development, using macromolecular crowding, *Tissue Eng Part A* 21(1-2) (2015) 183-92.
- [77] S. Werner, T. Krieg, H. Smola, Keratinocyte-fibroblast interactions in wound healing, *J Invest Dermatol* 127(5) (2007) 998-1008.
- [78] A. Konig, L. Bruckner-Tuderman, Transforming growth factor-beta promotes deposition of collagen VII in a modified organotypic skin model, *Lab Invest* 70(2) (1994) 203-9.
- [79] P.B. Garvey, R.A. Martinez, D.P. Baumann, J. Liu, C.E. Butler, Outcomes of abdominal wall reconstruction with acellular dermal matrix are not affected by wound contamination, *J Am Coll Surg* 219(5) (2014) 853-64.
- [80] J.J. Diaz, Jr., A.M. Conquest, S.J. Ferzoco, D. Vargo, P. Miller, Y.C. Wu, R. Donahue, Multi-institutional experience using human acellular dermal matrix for ventral hernia repair in a compromised surgical field, *Arch Surg* 144(3) (2009) 209-15.
- [81] J.H. Patton, Jr., S. Berry, K.A. Kralovich, Use of human acellular dermal matrix in complex and contaminated abdominal wall reconstructions, *Am J Surg* 193(3) (2007) 360-3; discussion 363.
- [82] D.T. Luttkhuizen, M.C. Harmsen, M.J. Van Luyn, Cellular and molecular dynamics in the foreign body reaction, *Tissue Eng* 12(7) (2006) 1955-70.
- [83] C.A. Carruthers, C.L. Dearth, J.E. Reing, C.R. Kramer, D.H. Gagne, P.M. Crapo, O. Garcia, Jr., A. Badhwar, J.R. Scott, S.F. Badylak, Histologic characterization of

acellular dermal matrices in a porcine model of tissue expander breast reconstruction, *Tissue Eng Part A* 21(1-2) (2015) 35-44.

[84] F. Li, W. Li, S. Johnson, D. Ingram, M. Yoder, S. Badylak, Low-molecular-weight peptides derived from extracellular matrix as chemoattractants for primary endothelial cells, *Endothelium* 11(3-4) (2004) 199-206.

[85] D.M. Hoganson, G.E. Owens, E.M. O'Doherty, C.M. Bowley, S.M. Goldman, D.O. Harilal, C.M. Neville, R.T. Kronengold, J.P. Vacanti, Preserved extracellular matrix components and retained biological activity in decellularized porcine mesothelium, *Biomaterials* 31(27) (2010) 6934-40.

[86] M.P. Lutolf, J.A. Hubbell, Synthetic biomaterials as instructive extracellular microenvironments for morphogenesis in tissue engineering, *Nat Biotechnol* 23(1) (2005) 47-55.

[87] M. Ehrbar, S.C. Rizzi, R.G. Schoenmakers, B.S. Miguel, J.A. Hubbell, F.E. Weber, M.P. Lutolf, Biomolecular hydrogels formed and degraded via site-specific enzymatic reactions, *Biomacromolecules* 8(10) (2007) 3000-7.

[88] P. Macchiarini, P. Jungebluth, T. Go, M.A. Asnaghi, L.E. Rees, T.A. Cogan, A. Dodson, J. Martorell, S. Bellini, P.P. Parnigotto, S.C. Dickinson, A.P. Hollander, S. Mantero, M.T. Conconi, M.A. Birchall, Clinical transplantation of a tissue-engineered airway, *Lancet* 372(9655) (2008) 2023-30.

[89] Q. Xing, K. Yates, M. Tahtinen, E. Shearier, Z. Qian, F. Zhao, Decellularization of fibroblast cell sheets for natural extracellular matrix scaffold preparation, *Tissue Eng Part C Methods* 21(1) (2015) 77-87.

[90] M. Peck, D. Gebhart, N. Dusserre, T.N. McAllister, N. L'Heureux, The evolution of vascular tissue engineering and current state of the art, *Cells Tissues Organs* 195(1-2) (2012) 144-58.

[91] C.A. Jahoda, K.A. Horne, A. Mauger, S. Bard, P. Sengel, Cellular and extracellular involvement in the regeneration of the rat lower vibrissa follicle, *Development* 114(4) (1992) 887-97.

[92] J.M. Aamodt, D.W. Grainger, Extracellular matrix-based biomaterial scaffolds and the host response, *Biomaterials* 86 (2016) 68-82.

[93] K.L. Ho, M.N. Witte, E.T. Bird, 8-ply small intestinal submucosa tension-free sling: spectrum of postoperative inflammation, *J Urol* 171(1) (2004) 268-71.